

**Development of Aircraft Fuel Burn Modeling Techniques
with Applications to Global Emissions Modeling
and Assessment of the Benefits of Reduced Vertical Separation Minimums**

by

Tim Yoder

B.S. Aeronautical and Astronautical Engineering
Ohio State University, 2005

SUBMITTED TO THE DEPARTMENT OF AERONAUTICS AND ASTRONAUTICS
IN PARTIAL FULFILLMENT OF THE REQUIREMENTS FOR THE DEGREE OF

MASTER OF SCIENCE IN AERONAUTICS AND ASTRONAUTICS
AT THE
MASSACHUSETTS INSTITUTE OF TECHNOLOGY

MAY 2007

[June 2007]

© 2007 Massachusetts Institute of Technology. All rights reserved.

The author hereby grants to MIT permission to reproduce
and to distribute publicly paper and electronic
copies of this thesis document in whole or in part.

Signature of Author.....



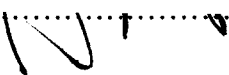
.....
Department of Aeronautics and Astronautics
May 2007

Certified by.....

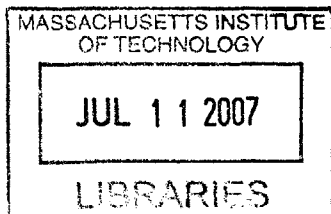


.....
Ian Waitz
Jerome C. Hunsaker Professor
Aeronautics and Astronautics
Thesis Supervisor

Accepted by.....



.....
Jaime Peraire
Professor of Aeronautics and Astronautics
Chairman, Committee for Graduate Students



AERO

**Development of Aircraft Fuel Burn Modeling Techniques
with Applications to Global Emissions Modeling
and Assessment of the Benefits of Reduced Vertical Separation Minimums**

by
Tim Yoder

Submitted to the Department of Aeronautics and Astronautics
on May 25, 2007 in Partial Fulfillment of the
Requirements for the Degree of Master of Science in
Aeronautics and Astronautics
At the Massachusetts Institute of Technology

ABSTRACT

Given the current level of concern over anthropogenic climate change and the role of commercial aviation in this process, the ability to adequately model and quantify fuel burn and emissions on a system wide scale is of high importance. In particular, the ability to adequately assess the ability of operational alternatives within the commercial aviation system to improve system efficiency and reduce environmental impact is essential.

Much work has already been done with this end in mind; however, given the high degree of complexity associated with a large system such as this, there is opportunity for improvements in modeling capability. The work presented in this thesis was conducted with this aim, to build additional functionality and fidelity into an established modeling method. The FAA System for assessing Aviation's Global Emissions (SAGE) is a well established model for the creation of global inventories of aviation fuel use and emissions. There are, however, two aspects of the model which could benefit from improvements in modeling methodology.

The first is the way in which the specific fuel consumption (SFC) is calculated. Previous to this study, SFC was calculated through the methods put forward in EUROCONTROL's Base of Aircraft Data (BADA). These methods are based on aircraft type specific coefficients and perform well in the context of global inventories; however, they lack the necessary functional dependence on ambient and operational variables to adequately assess the effects of the small changes often associated with various operational alternatives. An effort was made to assess the functional dependence of SFC on these variables through statistical analysis of a large body of Computerized Flight Recorder Data (CFDR) and to use this as a basis for improving the modeling of SFC in SAGE. The result of this effort was the introduction of a statistically-derived SFC model into SAGE which contained the desired functional dependence on temperature, pressure, Mach number, and thrust, and thereby improved the fidelity with which fuel burn is modeled. This SFC model, as implemented in SAGE, reduced the average absolute error by 21% as compared to the original BADA model.

Additional improvement was made with the introduction of weather information into the SAGE model. Previously, the model assumed standard atmospheric conditions and zero wind. An algorithm was devised which processed and incorporated global assimilated weather data from NASA Goddard into the performance calculations within SAGE. It was found that

the introduction of dynamic weather contributed greatly to the accuracy of SAGE given that the system wide average true airspeed error is 10% when the assumption of zero winds is used.

Finally this improved model was used to quantify the benefits of implementing Reduced Vertical Separation Minimums (RVSM) in US airspace in January of 2005. This was accomplished through a comparison of system wide efficiency during representative time periods prior to and following RVSM implementation. The results of this analysis provide insight into not only the benefits of RVSM, but also the effects of these model improvements and the efficacy of the different efficiency metrics used. It was found that RVSM resulted in an increase in fuel efficiency (nm/kg) of 1.81% ($\pm 0.55\%$) and an increase in NOx efficiency (nm/kg) of 3.14% ($\pm 1.25\%$). An additional control comparison was made, during these same time periods, of system efficiency over the North Atlantic and Western Europe where RVSM had been implemented several years prior. Using an efficiency metric which normalized for the difference in winds between the two periods it was found that there was indeed no benefit seen in this control study providing support for the US Domestic RVSM results.

Thesis Supervisor:

Ian Waitz

Title:

Jerome C. Hunsaker Professor
Aeronautics and Astronautics

ACKNOWLEDGEMENTS

I would first like to thank Professor Ian Waitz for his counsel and support throughout this endeavor. He was always available with thoughtful guidance despite the many demands on his time, and my morale was constantly fortified by the contagious enthusiasm he brings to his work.

Next, I would like to thank the Volpe National Transportation Systems Center. The time and efforts of Gregg Fleming, Sathya Balasubramanian, Andrew Malwitz, and numerous others were critical to the completion of this study. I am most appreciative of the many hours of support they provided in furtherance of this research.

I would also like to thank everyone at the Goddard Earth Sciences (GES) Data and Information Services Center (DISC) Distributed Active Archive Center (DAAC) for their assistance in attaining the weather data used in this study.

Finally, I would like to thank everyone else that I have had the pleasure of interacting with during the course of these last several years. The myriad creative ideas and valuable feedback you have provided are greatly appreciated, and your friendship and collaboration are genuinely cherished.

This work was supported by the Office of Environment and Energy, U.S. Federal Aviation Administration under Contract No. DTFAWA-05-D-00012, Task Order 0001 managed by Warren Gillette and Task Order 0005 managed by Maryalice Locke, and by the Environmental Measurement and Modeling Division of the Research and Special Programs Administration, Volpe National Transportation Systems Center, U.S. Department of Transportation under Contract Nos. DTRS57-05-P-80103 and DTRT57-05-P-80126 managed by Gregg Fleming and Clay Reherman. Any opinions, findings, and conclusions or recommendations expressed in this material are those of the author(s) and do not necessarily reflect the views of the FAA or DoT.

CONTENTS

- CHAPTER 1: INTRODUCTION..... 9**
- CHAPTER 2: MODEL DEVELOPMENT 11**
 - 2.1. SAGE OVERVIEW 11
 - 2.1.1. *Purpose* 11
 - 2.1.2. *Model Structure* 12
 - 2.1.3. *Basic Algorithm Description* 13
 - 2.2. FUEL BURN MODEL DEVELOPMENT 15
 - 2.2.1. *Purpose* 15
 - 2.2.2. *Approach*..... 15
 - 2.2.3. *Results*..... 19
 - 2.2.4. *Implementation* 23
 - 2.3. INCLUSION OF METEOROLOGICAL INFORMATION 31
 - 2.3.1. *Purpose* 31
 - 2.3.2. *Approach*..... 31
 - 2.3.3. *Implementation* 32
 - 2.3.4. *Results*..... 33
- CHAPTER 3: MODEL APPLICATION 36**
 - 3.1. RVSM BENEFIT ASSESSMENT 36
 - 3.1.1. *Purpose* 36
 - 3.1.2. *Previous Studies of RVSM* 37
 - 3.1.3. *Approach*..... 38
 - 3.1.4. *Results*..... 44
 - 3.1.5. *Conclusions*..... 47
- APPENDIX A: EXAMPLE 48**
 - A.1. TRANSONIC DRAG CORRECTION 48

LIST OF FIGURES

FIGURE 2.1 – SAGE GLOBAL FUEL BURN INVENTORIES FOR 2000.....	11
FIGURE 2.2 – SCHEMATIC OF SAGE MODEL STRUCTURE ²	12
FIGURE 2.3 – EXAMPLE OF NET THRUST CALCULATION	17
FIGURE 2.4 – NON-DIMENSIONAL ANALYSIS OF RB211 TURBOFAN ⁹	18
FIGURE 2.5 – SFC MODEL ERROR COMPARISON	20
FIGURE 2.6 – EXAMPLE COMPARISON OF FUEL BURN RATE (B757-200).....	21
FIGURE 2.7 – EXAMPLE COMPARISON OF SFC MODELS (B757-200)	21
FIGURE 2.8 – EXAMPLE COMPARISON OF FUEL BURN RATE (RJ85).....	22
FIGURE 2.9 – EXAMPLE COMPARISON OF SFC MODELS (RJ85)	22
FIGURE 2.10 – COMPARISON OF CFDR AND BADA DERIVED α VALUES.....	23
FIGURE 2.11 – COMPARISONS OF CORRECTED AND ORIGINAL BADA SFC TO CFDR DATA (A319)	25
FIGURE 2.12 – COMPARISONS OF CORRECTED AND ORIGINAL BADA SFC TO CFDR DATA (A320-214).....	25
FIGURE 2.13 – COMPARISONS OF CORRECTED AND ORIGINAL BADA SFC TO CFDR DATA (A321)	26
FIGURE 2.14 – COMPARISONS OF CORRECTED AND ORIGINAL BADA SFC TO CFDR DATA (A330-202).....	26
FIGURE 2.15 – COMPARISONS OF CORRECTED AND ORIGINAL BADA SFC TO CFDR DATA (A330-243).....	27
FIGURE 2.16 – COMPARISONS OF CORRECTED AND ORIGINAL BADA SFC TO CFDR DATA (A330-223).....	27
FIGURE 2.17 – COMPARISONS OF CORRECTED AND ORIGINAL BADA SFC TO CFDR DATA (A340-300).....	28
FIGURE 2.18 – COMPARISONS OF CORRECTED AND ORIGINAL BADA SFC TO CFDR DATA (A340-500).....	28
FIGURE 2.19 – COMPARISONS OF CORRECTED AND ORIGINAL BADA SFC TO CFDR DATA (B757-200)	29
FIGURE 2.20 – COMPARISONS OF CORRECTED AND ORIGINAL BADA SFC TO CFDR DATA (B767-300)	29
FIGURE 2.21 – COMPARISONS OF CORRECTED AND ORIGINAL BADA SFC TO CFDR DATA (B777-300ER)...	30
FIGURE 2.22 – COMPARISONS OF CORRECTED AND ORIGINAL BADA SFC TO CFDR DATA (RJ85)	30
FIGURE 2.23 – COMPARISON OF GEOS WIND MAGNITUDE TO CFDR DATA.....	34
FIGURE 2.24 – COMPARISON OF GEOS WIND DIRECTION TO CFDR DATA.....	34
FIGURE 2.25 – COMPARISON OF GEOS TEMPERATURE TO CFDR DATA	35
FIGURE 2.26 – COMPARISON OF GEOS PRESSURE TO CFDR DATA	35
FIGURE 3.1 – RVSM IMPLEMENTATION SCHEDULE ¹⁷	36
FIGURE 3.2 – CRUISE ALTITUDE WINDS DURING PRE-RVSM STUDY PERIOD.....	40
FIGURE 3.3 – CRUISE ALTITUDE WINDS DURING POST-RVSM STUDY PERIOD.....	40
FIGURE 3.4 – US DOMESTIC PRE RVSM ETMS DATA POINTS.....	42
FIGURE 3.5 – US DOMESTIC POST RVSM ETMS DATA POINTS.....	42
FIGURE 3.6 – NORTH ATLANTIC AND E.U. PRE RVSM ETMS DATA POINTS	43
FIGURE 3.7 – NORTH ATLANTIC AND E.U. POST RVSM ETMS DATA POINTS	43
FIGURE 3.8 – US DOMESTIC RVSM ANALYSIS RESULTS.....	44
FIGURE 3.9 – NORTH ATLANTIC AND E.U. (CONTROL) RVSM ANALYSIS RESULTS.....	45

LIST OF TABLES

TABLE 2.1– CFDR DATA COMPOSITION.....	15
TABLE 2.2– CFDR DATA TEMPORAL RESOLUTION	16
TABLE 2.3– RESULTS OF CFDR STATISTICAL ANALYSIS	19
TABLE 3.1– DATES EXAMINED IN RVSM STUDY ¹⁵	38
TABLE 3.2– US DOMESTIC RVSM ANALYSIS RESULTS.....	44
TABLE 3.3– US DOMESTIC MONTHLY LOAD FACTORS.....	46

NOMENCLATURE

Constants

g Acceleration of gravity ($9.81 \frac{m}{s^2}$)

Variables

ΔC_{dc} Transonic drag correction

C_L Lift coefficient

M Mach number

S Wing surface area

SFC Specific fuel consumption

T Thrust

D Drag

C_{d0} Parasitic drag coefficient in BADA

C_{d2} Induced drag coefficient in BADA

C_{f1} Fuel flow coefficient in BADA #1

C_{f2} Fuel flow coefficient in BADA #2

C_{fer} Cruise fuel flow coefficient in BADA

M_{BC} BADA cruise Mach number

V Velocity

ΔX Distance

m Mass

h Altitude

t Time

ρ Density

θ Ratio of ambient temperature to sea level standard

δ Ratio of ambient pressure to sea level standard

τ Ratio of thrust to sea level maximum

\dot{m}_f Fuel burn rate

m_f Fuel burn

m_p Mass of payload

η Efficiency

GLOSSARY

BADA - Base of Aircraft Data

BFFM2 - Boeing Fuel Flow Method 2

CFDR - Computer Flight Data Recorder

EI - Emissions Indices

ETMS - Enhanced Traffic Management System

FAA - Federal Aviation Administration

GEOS - Goddard Earth Observing System

MIT - Massachusetts Institute of Technology

NAS – National Airspace System

NASA - National Air and Space Administration

PDARS - Performance Data Analysis and Reporting System

SAGE - System for Assessing Global Emissions

SFC - Specific Fuel Consumption

VOLPE - Volpe National Transportation Systems Center, Environmental Measurements and Modeling Division

CHAPTER 1: Introduction

Given the negative environmental impacts associated with the use of fossil fuels for transportation, it is important to seek methods for reducing the use of these fuels and the emissions they produce. Also, due to the mass and volume constraints associated with aircraft design, hydrocarbon fuels are likely to remain the primary energy source in this sector for some time, even as alternative fuels become more prevalent in ground transport applications. It is estimated that commercial aviation currently accounts for about 3% of global oil consumption and fuel use is projected to grow at a rate of 3% per year through 2015.¹ It is therefore critical to develop a modeling and analysis capabilities which can be used to estimate historical fuel usage as well as to assess the utility of various operational alternatives in reducing future fuel use and emissions.

The purpose of the work described in this thesis is that of model enhancement, followed by the application of that improved model in the assessment of an operational initiative to improve air transportation system efficiency. The process of model enhancement builds upon previous work done in this area and utilizes the FAA's System for assessing Aviations Global Emissions (SAGE) as the base model. This thesis will first provide a summary of the modeling algorithm employed by SAGE, followed by a description of two recent enhancements made to that algorithm. Finally, the results of the application of this model to the assessment of the benefits of Reduced Vertical Separation Minimums (RVSM) in US airspace are discussed.

The first of the model improvements was the derivation and implementation of a fuel burn model which provides the functional dependencies necessary to more accurately assess the benefits of operational alternatives in the aviation system. The previous fuel burn modeling method in SAGE contained dependencies on only velocity and altitude, whereas theory predicts a dependence upon additional variables such as Mach number, ambient temperature and pressure, and engine operating point. A large body of empirical data was analyzed to determine the appropriate dependencies on these additional variables and a method was devised for incorporating this additional fuel burn functionality into SAGE.

Additionally, it was necessary to devise a means of incorporating weather information into SAGE. Previously, SAGE assumed standard atmospheric conditions and no winds. The inclusion of weather information was particularly important in light of the newly incorporated dependence of fuel burn on ambient conditions. The ability to include winds is also of great importance to model fidelity, as was evidenced by the RVSM analysis. Using global assimilated weather data from NASA Goddard, an algorithm for preprocessing and incorporating weather information into the SAGE model was developed.

This enhanced version of SAGE was then used to investigate the benefits of the implementation of RVSM in US domestic airspace. The results of this investigation indicate that the system wide benefits of RVSM are substantial in terms of fuel burn and emissions reduction as will be described further in Chapter 3.

CHAPTER 2: Model Development

2.1. SAGE Overview

SAGE was originally developed for the FAA by a collaboration of the Volpe National Transportation Systems Center (Volpe), the Massachusetts Institute of Technology (MIT), and the Logistics Management Institute (LMI). Much of the research presented in this thesis involves either the introduction of enhancements into SAGE or the assessment of operational alternatives using SAGE. Thus a brief description of the fundamental algorithms used in SAGE is presented here, with particular emphasis on those aspects that are directly related to the present research. A more thorough explanation can be found in the SAGE Technical Manual².

2.1.1. Purpose

The fundamental purpose of SAGE is to serve as a modeling tool which is capable of taking as input flight trajectory information and producing as output an inventory of the fuel burn and emissions produced by those flights. The tool is currently used for the production of annual global fuel burn inventories for the FAA and for the assessment of various policy scenarios. Figure 2.1 depicts an example global fuel burn inventory for 2000 as produced by SAGE.

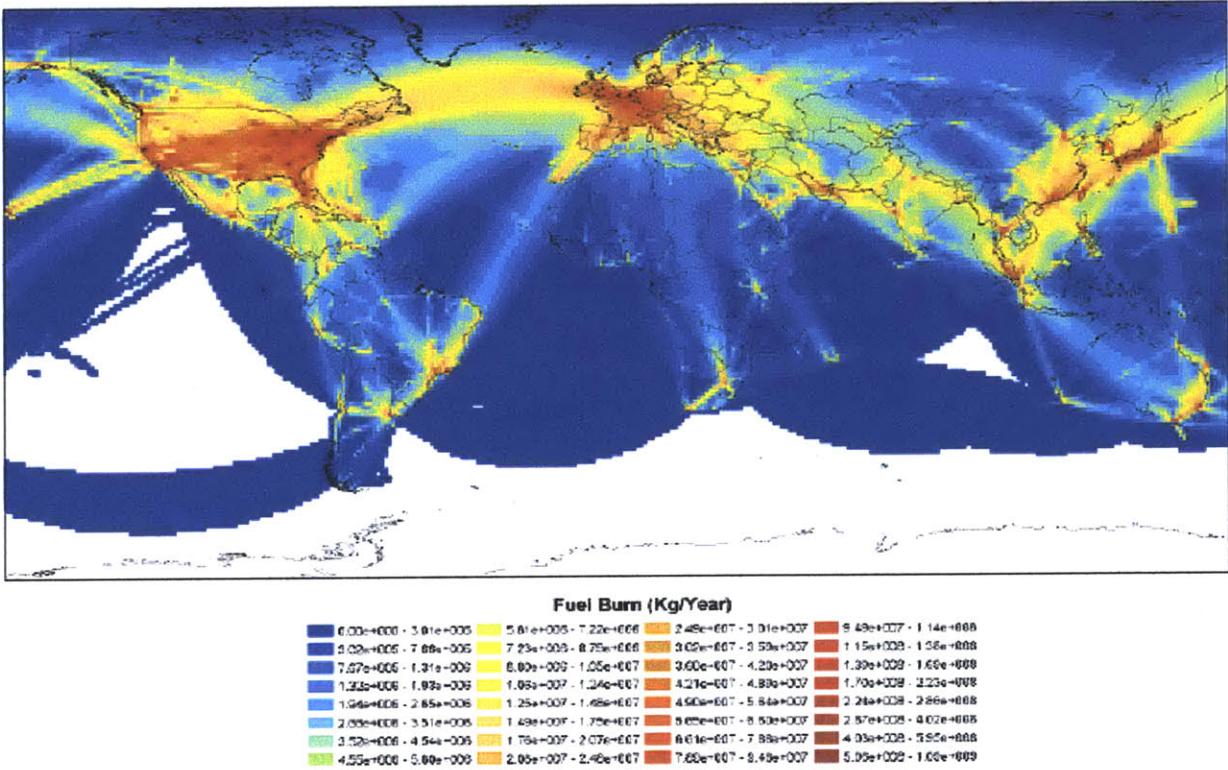


Figure 2.1 – SAGE Global Fuel Burn Inventories for 2000

2.1.2. Model Structure

The structure of SAGE is modular, which allows changes to be implemented with relative ease. Figure 2.2 depicts the general structure of SAGE; however, it should be noted that the forecasting capabilities of SAGE were not utilized at any time in this particular study.

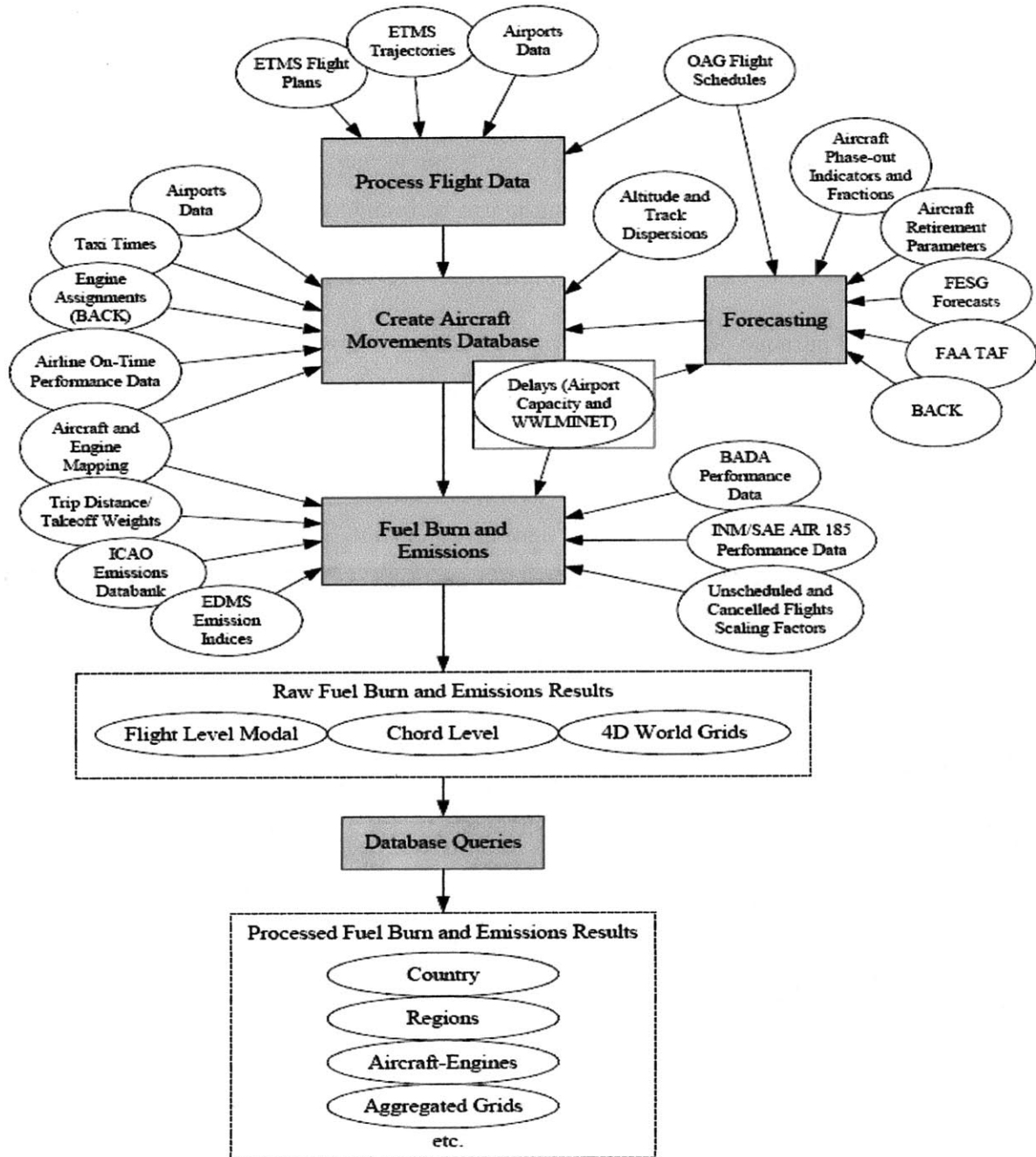


Figure 2.2 – Schematic of SAGE Model Structure²

2.1.3. Basic Algorithm Description

The basic flow of information within SAGE begins with the input of flight trajectory information. SAGE is capable of accepting as input both detailed radar-based trajectory information and listings of origin destination pairs when radar data is unavailable. In the later case the trajectories are generated within SAGE based on a stochastic dispersion about a great circle flight path. The radar-based trajectories are filtered to remove any anomalous points resulting from radar station overlap. For this particular study, the inputs were only radar based trajectories as archived within the FAA's Enhanced Traffic Management System³ (ETMS).

The next step is to model the thrust necessary to realize the flight paths depicted in the ETMS trajectories. This is accomplished through the enforcement of energy conservation as the aircraft moves between consecutive data points. Consecutive points along the trajectory are connected by straight line chords for which the following performance data are available.

- 1) V Average velocity
- 2) ΔV Change in velocity along chord
- 3) m Gross mass of aircraft
- 4) h Average altitude
- 5) Δh Change in altitude along chord
- 6) Δt Elapsed time

Using this information, the coefficient of lift, C_L , is calculated for a chord.

$$C_L = \frac{2mg}{\rho V^2 S}$$

The drag coefficient, C_D , is then determined using aircraft type specific coefficients contained in EUROCONTROL's **Base of Aircraft Data**⁴ (BADA) along with a correction for transonic drag rise, ΔC_{ac} . The transonic drag correction is modeled as a piecewise defined third order polynomial, the definition of which is given in appendix A.1.

$$C_D = C_{d0} + C_{d2}(C_L)^2 + \Delta C_{ac}$$

The drag along a chord, D , is then calculated.

$$D = \frac{1}{2} \rho V^2 C_D S$$

By enforcing the conservation of energy the net thrust, T , necessary to achieve the trajectory of a chord is then calculated.

$$T = D + \frac{mg}{V} \frac{\Delta h}{\Delta t} + m \frac{\Delta V}{\Delta t}$$

The SFC is then attained through the following algorithm as defined in BADA.

If $h \leq 7620m$

$$SFC = \frac{C_{f1}}{6000} \left(1 + \frac{1.9438V}{C_{f2}} \right)$$

If $h > 7620m$

$$SFC = \frac{C_{f1}}{6000} \left(1 + \frac{1.9438V}{C_{f2}} \right) C_{fcr}$$

Where C_{f1} and C_{f2} are aircraft type specific coefficients contained in BADA and C_{fcr} is an aircraft type specific altitude correction factor. It should be noted that this method of computing SFC reflects only a linear dependence on velocity and a discontinuous step dependence on altitude.

The fuel burn rate, \dot{m}_f , is then calculated from the thrust and SFC.

$$\dot{m}_f = (T)(SFC)$$

The total fuel burn for the chord is then calculated.

$$m_f = \dot{m}_f \Delta t$$

The fuel burn along the chord is then debited from the aircraft mass and the process is repeated for the following chord. Additionally, the emissions along each chord are calculated using the fuel burn information, Boeing Fuel Flow Method 2⁵ (BFFM2), and engine type specific ICAO Emissions Indices⁶ (EI). The algorithm for the calculation of emissions is laid out in detail in the SAGE technical manual.

Thus the fuel burn and emissions are calculated for each chord of the flight and these results are aggregated for all flights being considered in a particular study.

2.2. Fuel Burn Model Development

The development of high fidelity fuel burn models for use within SAGE was accomplished through the analysis of empirical data within the context of theoretically predicted functional dependencies.

2.2.1. Purpose

Prior to the development of these improved fuel burn models, the fuel burn modeling method employed in SAGE was based on BADA coefficients as described in section 2.1.3. This method lacks the functional dependencies on ambient and operating conditions that are necessary to evaluate the benefits of various operational alternatives. Often the benefits resulting from the implementation of operational alternatives are relatively small and it is therefore necessary to make use of the highest fidelity models possible in evaluating any potential benefits.

2.2.2. Approach

The approach taken toward model development was to make use of empirical data on engine performance during flight to create a model which best reflects the in situ fuel burn. To this end a large body of computerized flight data recorder⁷ (CFDR) data was obtained for a variety of commercial aircraft. Table 2.1 provides a breakdown of the aircraft and engine types represented in this data set, as well as the operating airline and number of representative flights for each.

Table 2.1– CFDR Data Composition

Aircraft Type	Engine Type	Airline	Number of flights
A319	CFM56-5B5-2	Swiss	191
A320-214	CFM56-5B4-2	Swiss	240
A321	CFM56-5B1-2	Swiss	176
A330-202	PW4168	Etihad	224
A330-243	RR Trent 700	Etihad	238
A330-223	PW4168A	Swiss	264
A340-300	CFM56-5C4/P	Swiss	188
A340-500	RR Trent 500	Etihad	262
B757-200	RB211-535C	Bel Air	178
B767-300	CF6-80C2	Etihad	222
B777-300ER	GE90-115B1	Etihad	365
AR85	LF 507-1F	Swiss	266

The CFDR data were quite extensive in the breadth of variables contained, with 103 directly measured or derived values. Of interest to this study in particular were the following variables.

- 1) Ambient Temperature
- 2) Ambient Pressure
- 3) Mach Number
- 4) Altitude
- 5) Fuel flow
- 6) Gross Mass

The values of these variables were represented at a temporal resolution which varied dependent upon the mode of flight as defined in table 2.2.

Table 2.2– CFDR Data Temporal Resolution

Mode	Δt (sec)
Take off and Climb (below 5000 ft)	1
Climb (above 5000 ft)	10
Cruise	150
Descent (above 5000 ft)	10
Descent and Landing (below 5000 ft)	1

The desired result of this analysis was a model of specific fuel consumption (SFC) which accurately reflects the effects of small changes in the following ambient and operating conditions.

- 1) Ambient Temperature
- 2) Ambient Pressure
- 3) Mach Number
- 4) Net Thrust

Theory indicates that these four variables are the dominant operational factors influencing SFC and they are all available as measured values in the CFDR data except the net thrust. It is, however, possible to derive the value of net thrust from the CFDR data through the use of the trajectory and mass information it contains. This was accomplished through the same techniques and assumptions currently used to calculate net thrust in SAGE. As described in section 2.1.3, this assumes acceptable accuracy of the type specific BADA drag coefficients used in the calculation of drag, D . This accuracy was previously found to be within $\pm 14\%$ of

corresponding NASA data with 1σ confidence⁸. It should be noted that these drag coefficients are supplied by the aircraft manufacturers for incorporation into the BADA database. An example of the net thrust, as derived for the B757-200 using this method, is depicted in figure 2.3.

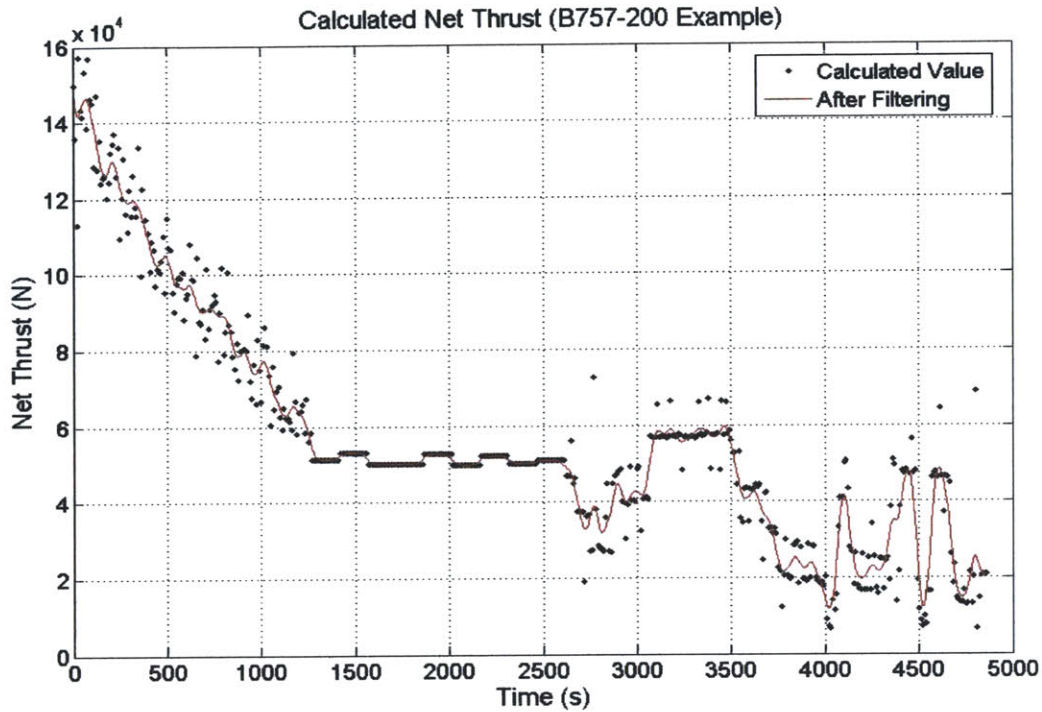


Figure 2.3 – Example of Net Thrust Calculation

As a result of the small Δt 's during certain portions of the flight this algorithm for computing net thrust often results in rapid thrust variations during these periods. The frequency of these is considerably greater than would be possible or expected given the inertia of the aircraft and it was therefore filtered out through the application of a three point moving average algorithm. An example output of this filtering can be seen in the solid red line in Figure 2.3.

With the relevant variables all available the process of discerning the functional dependence of SFC on those variables was conducted using statistical regression methods. The first step in this process was to determine the theoretically predicted form of the equation describing SFC. Dimensional analysis indicates that the relevant relation can be written in non-dimensional form as,

$$\frac{SFC}{\sqrt{\theta}} = f\left(M, \frac{N_g}{\sqrt{\theta}}, Re\right)$$

Results presented in Mechanics and Thermodynamics of Propulsion⁹ suggest that Reynolds number effects are not significant when compared to the effects of Mach number and shaft speed. Additionally, there is a non-dimensional relationship between shaft speed, temperature, pressure, and net thrust according to the relation,

$$\frac{N_g}{\sqrt{\theta}} = f\left(\frac{\tau}{\delta}\right)$$

This allows for a substitution resulting in the following relationship:

$$\frac{SFC}{\sqrt{\theta}} = f\left(M, \frac{\tau}{\delta}\right)$$

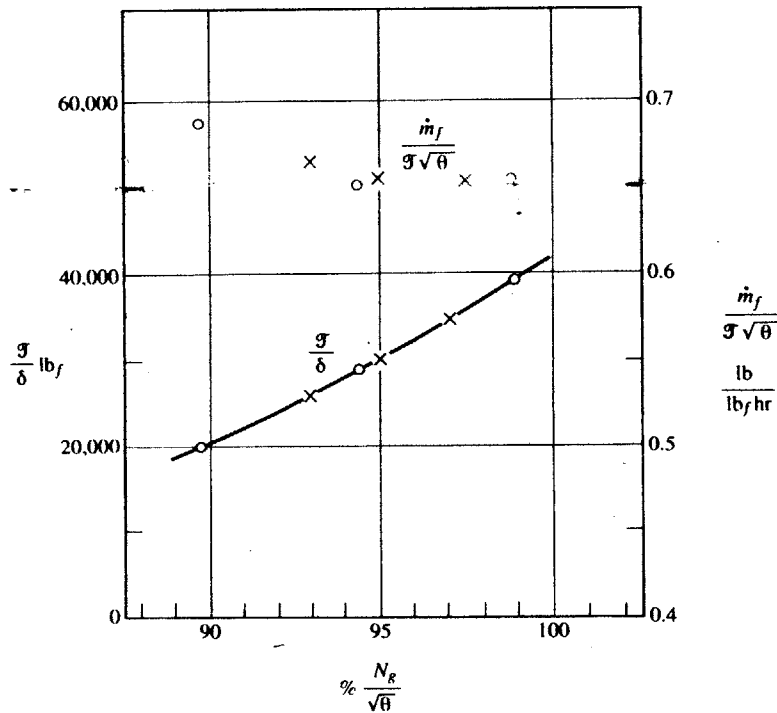


Figure 2.4 – Non-Dimensional Analysis of RB211 Turbofan⁹

According to an analysis presented in this same text and reproduced here in Figure 2.4, the general form of the dependence of $\frac{SFC}{\sqrt{\theta}}$ on $\frac{N_g}{\sqrt{\theta}}$ is exponential decay, and $\frac{N_g}{\sqrt{\theta}}$ varies

approximately as $\left(\frac{\tau}{\delta^{0.9}}\right)^{0.3}$. These theoretically predicted relationships were considered in the construction of the form for SFC used as a prior for the statistical data fitting process. A large number of variations of the form of the equation for SFC were tested before arriving at a form which provided the best performance. This best form was determined to be the following.

$$\frac{SFC}{\sqrt{\theta}} = \alpha + \beta_1 M + \beta_2 e^{-\beta_3 \left(\frac{\tau}{\delta^{0.9}}\right)^{0.3}}$$

The values of the α and β coefficients in this equation were then determined through the iterative application of a least squared error algorithm. This was necessary given the fact that the equation contains both a linear and exponential functionality on the unknown coefficients. The approach was to iterate on β_3 , and with each iteration solve for the least squared error estimates of the remaining unknowns. This process eventually converged to a solution for all the coefficients which minimized the difference between the predicted SFC and that contained in the CFDR data.

2.2.3. Results

This analysis was carried out for each of the aircraft types in Table 2.1 and the resultant best fit values of the coefficients are given here in Table 2.3.

Table 2.3– Results of CFDR Statistical Analysis

Type	α	β_1	β_2	β_3
A319	1.25E-05	5.03E-06	1.64E-04	6.40E+00
A320-214	1.13E-05	7.84E-06	1.46E-04	5.70E+00
A321	1.26E-05	5.47E-06	1.63E-04	6.50E+00
A330-202	1.11E-05	7.46E-06	6.79E-05	5.00E+00
A330-243	1.05E-05	8.61E-06	2.18E-04	8.00E+00
A330-223	1.05E-05	8.38E-06	1.47E-04	7.50E+00
A340-300	1.26E-05	4.69E-06	3.19E-05	3.30E+00
A340-500	9.52E-06	8.38E-06	1.95E-04	6.60E+00
B757-200	1.04E-05	9.51E-06	8.84E-05	4.60E+00
B767-300	1.45E-05	2.87E-06	1.38E-04	8.90E+00
B777-300ER	1.24E-05	5.99E-06	3.10E-04	1.00E+01
ARJ85	6.84E-06	2.16E-05	3.64E-04	5.80E+00

These fitted coefficients provide for a noticeable improvement in fuel burn modeling capability when compared with BADA methods. This can be seen in the example flights depicted in

Figures 2.6 through 2.9, as well as the SFC comparisons for all 12 aircraft types depicted in Figures 2.11 through 2.22. These Figures provide a comparison of the type specific SFC models derived here, the generalized SFC model discussed later, and the original BADA SFC model. This comparison was accomplished through the application of each model to the CFDR data inputs and plotting the model output against the actual SFC value in the CFDR data. Thus, a perfect correspondence would lie along the red diagonal depicted in each graph.

Figure 2.5 depicts the mean absolute error in the estimates produced by the derived model and the BADA model. The derived SFC model led to a 41% average reduction in mean absolute error across all 12 aircraft types.

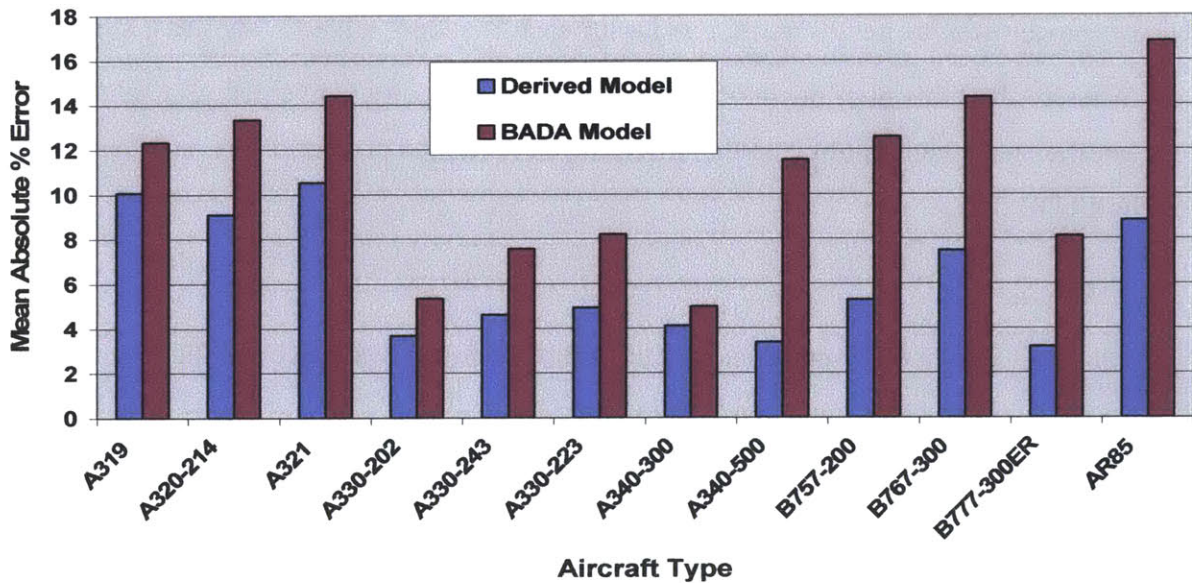


Figure 2.5 – SFC Model Error Comparison

While the fuel burn functionality is dominated by the amount of thrust required, the ability to capture the effects of ambient and operational factors is of significant value in improving the fidelity of SFC and the resultant fuel burn. In particular, it is important to accurately capture the sensitivity of SFC to these factors in order to assess the effects of small operational changes.

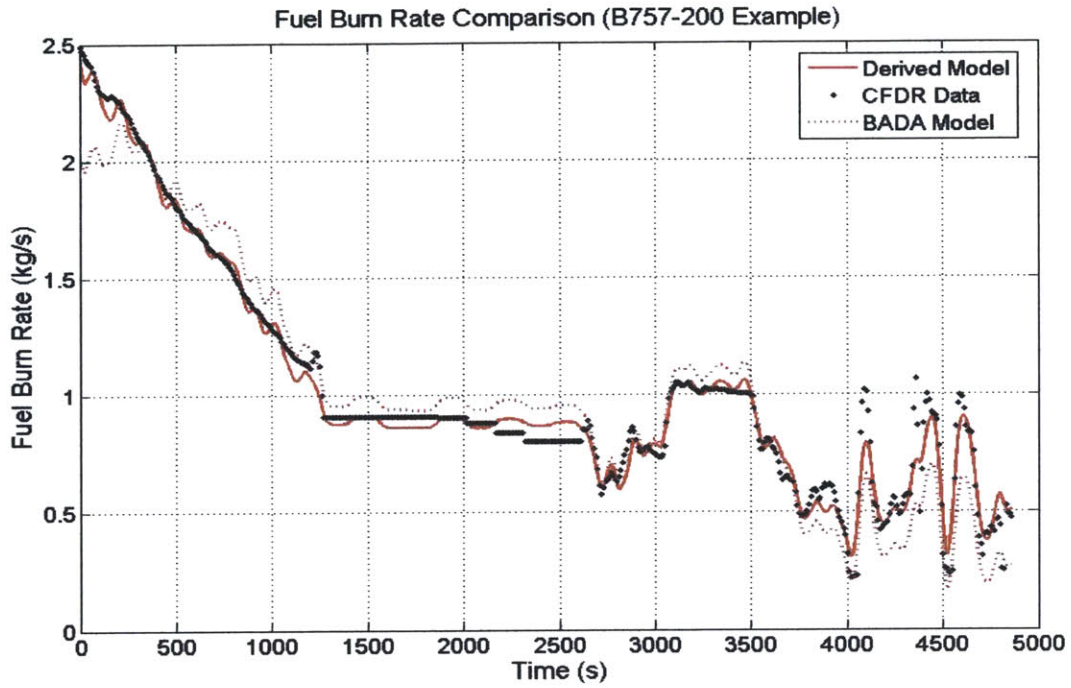


Figure 2.6 – Example Comparison of Fuel Burn Rate (B757-200)

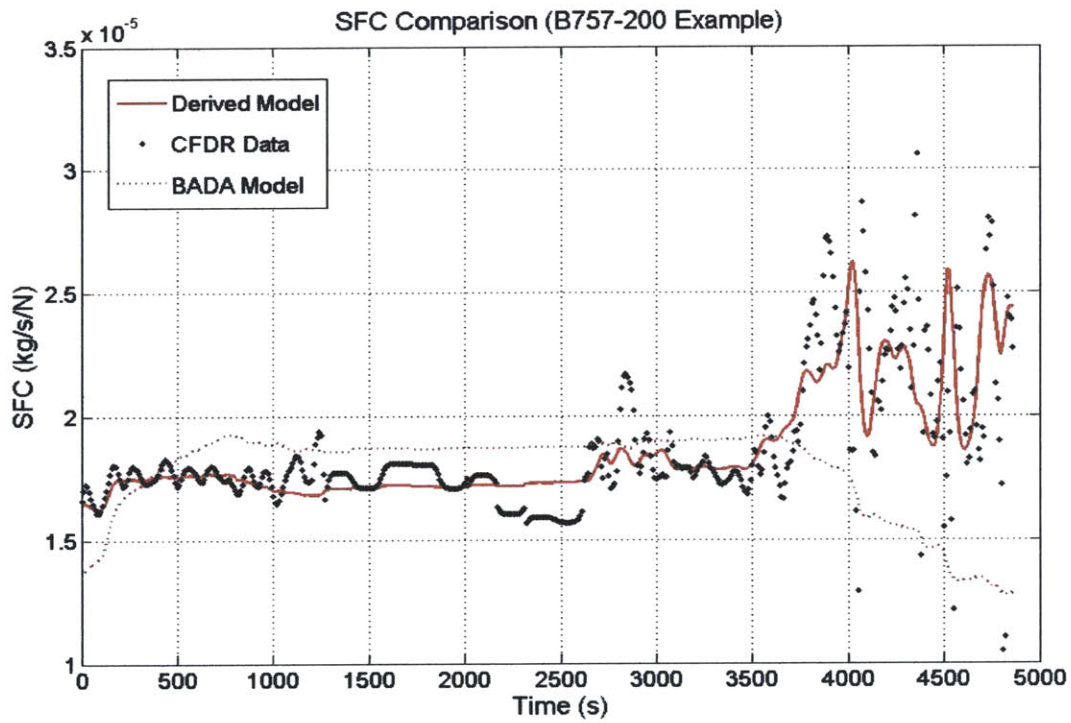


Figure 2.7 – Example Comparison of SFC Models (B757-200)

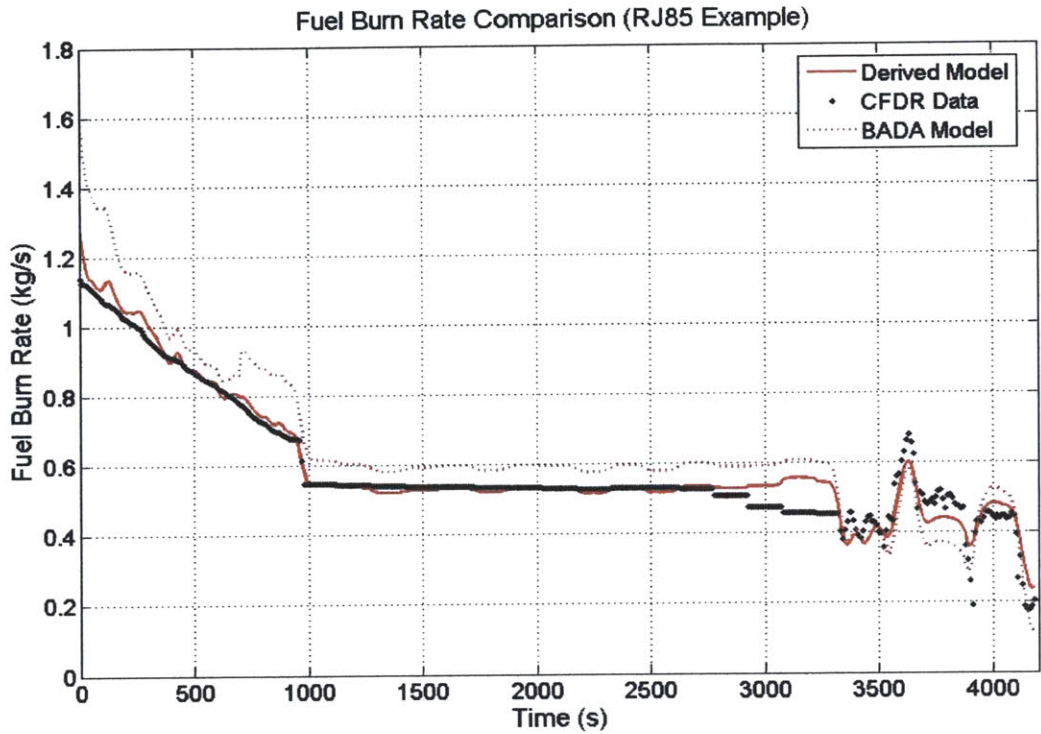


Figure 2.8 – Example Comparison of Fuel Burn Rate (RJ85)

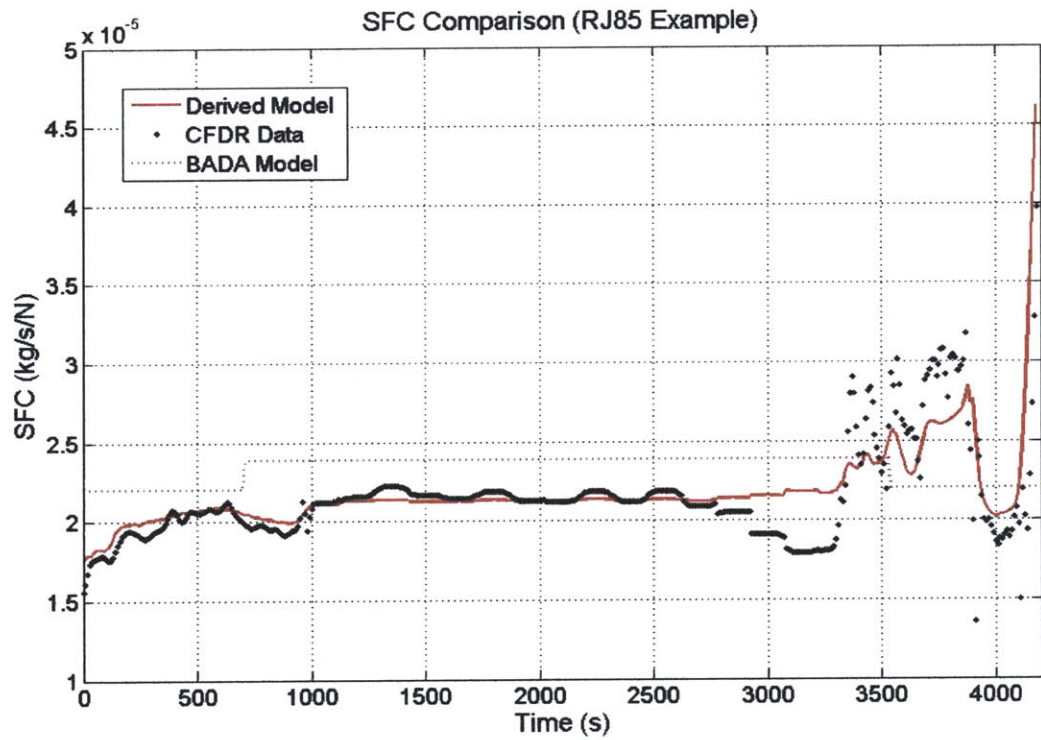


Figure 2.9 – Example Comparison of SFC Models (RJ85)

2.2.4. Implementation

In order to make use of these results within the context of SAGE, where a broad spectrum of aircraft types needs to be modeled, it was necessary to devise a means of generalizing the results for these aircraft to the fleet as a whole. The approach taken was to incorporate the common trends in SFC functionality into a correction to be applied to the BADA SFC model, as this model is available for all the necessary aircraft types. By forcing the values of the β coefficients to their common mean and solving for α it was found that there was a high degree of correlation between the CFDR derived α 's and the value of their respective BADA SFC coefficients. Figure 2.10 depicts a comparison of the values of α derived in this manner and a surrogate α derived entirely from BADA SFC coefficients based upon this correlation.

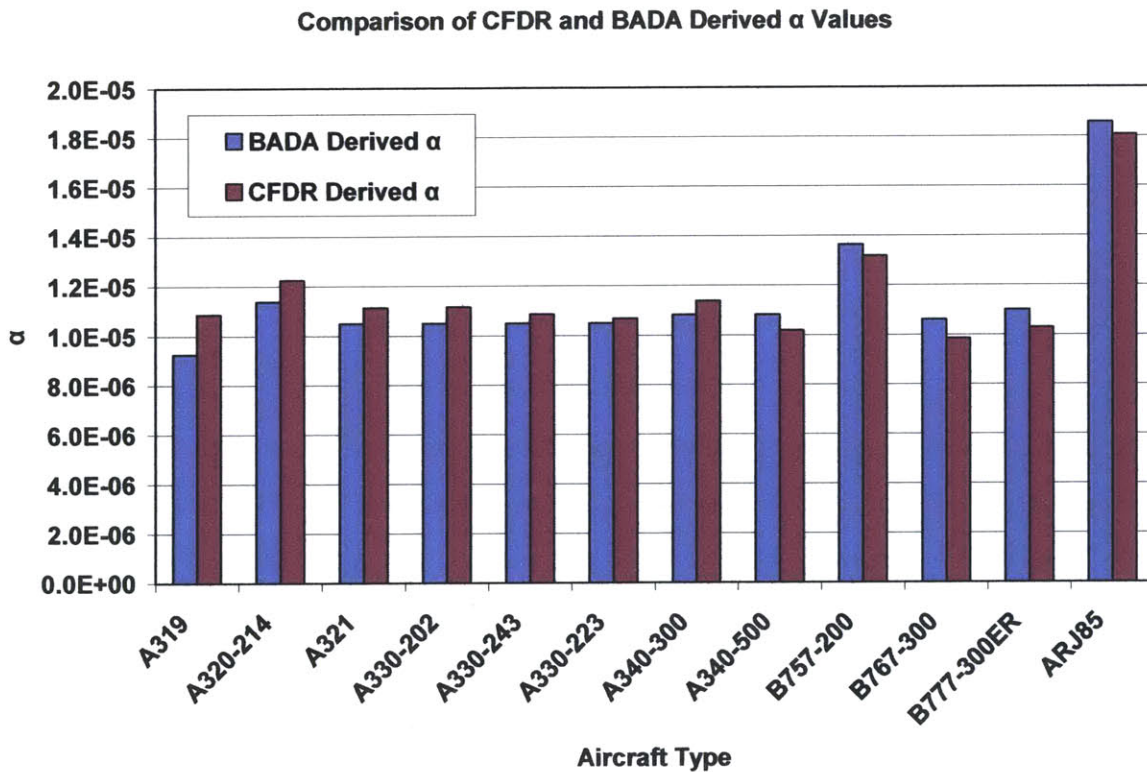


Figure 2.10 – Comparison of CFDR and BADA Derived α Values

This surrogate α is derived from the associated BADA coefficients through the following relation,

$$\alpha = \frac{C_{f1}}{60000} \left(1 + \frac{1.9438(240)}{C_{f2}} \right) C_{fer} - 5.3(10)^{-6}$$

Making use of this type specific surrogate α along with the mean value of the β coefficients, it was possible to create a new universally applicable SFC model based entirely upon BADA SFC coefficients and incorporating the functionality derived from the CFDR data. This model is defined as,

$$\frac{SFC}{\sqrt{\theta}} = \alpha + \beta_1 M + \beta_2 e^{-\beta_3 \left(\frac{\tau}{\delta^{0.9}} \right)^{0.3}}$$

With the mean β coefficients defined as,

$$\beta_1 = 7.70(10)^{-6}$$

$$\beta_2 = 1.86(10)^{-4}$$

$$\beta_3 = 6.75$$

This generally applicable model was then incorporated into SAGE with little difficulty since it requires only the BADA coefficients for input. The result is an ability to model all the required aircraft types in the commercial fleet with an improved fidelity for the effects of ambient and operating conditions. Figures 2.11 through 2.22 also depict SFC as estimated using this generalized derived method (central graphic) versus the SFC in the CFDR data. As can be seen in these figures the process of generalization diminishes the accuracy somewhat as compared with the type specific model, however, the mean absolute error is still reduced by an average of 21% compared to the original BADA method. Of particular importance, the general dependencies on those variables other than velocity are largely preserved; retaining the model's enhanced utility in evaluating operational alternatives.

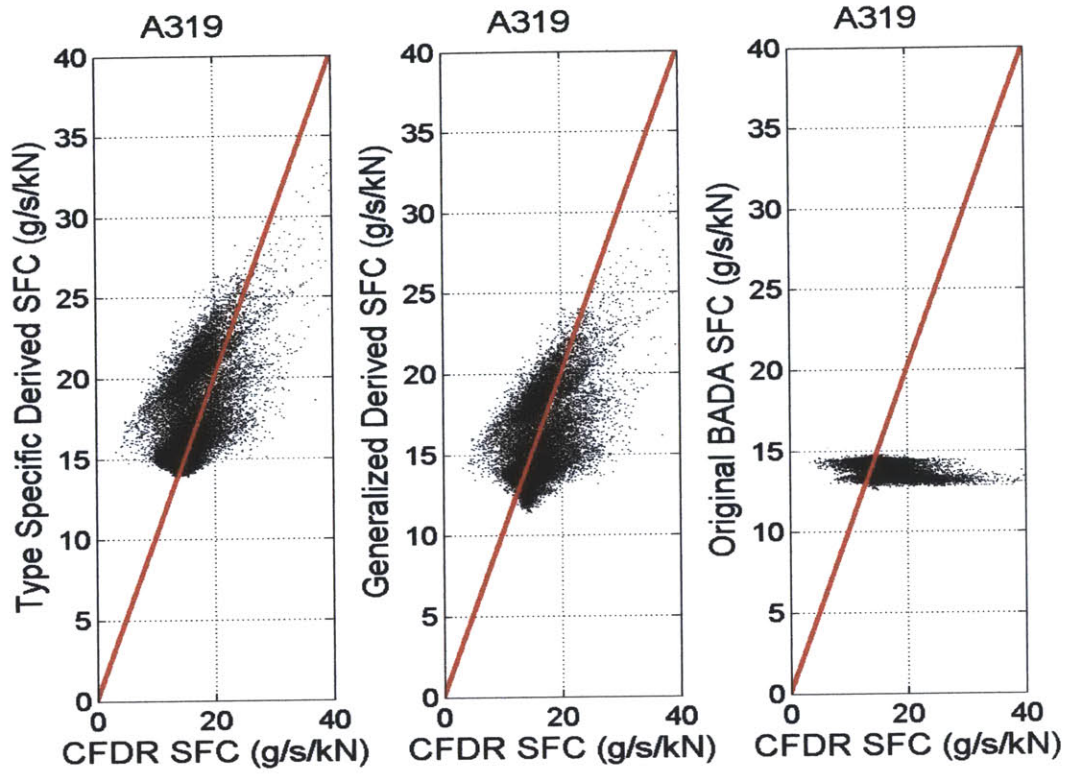


Figure 2.11 – Comparisons of Corrected and Original BADA SFC to CFDR Data (A319)

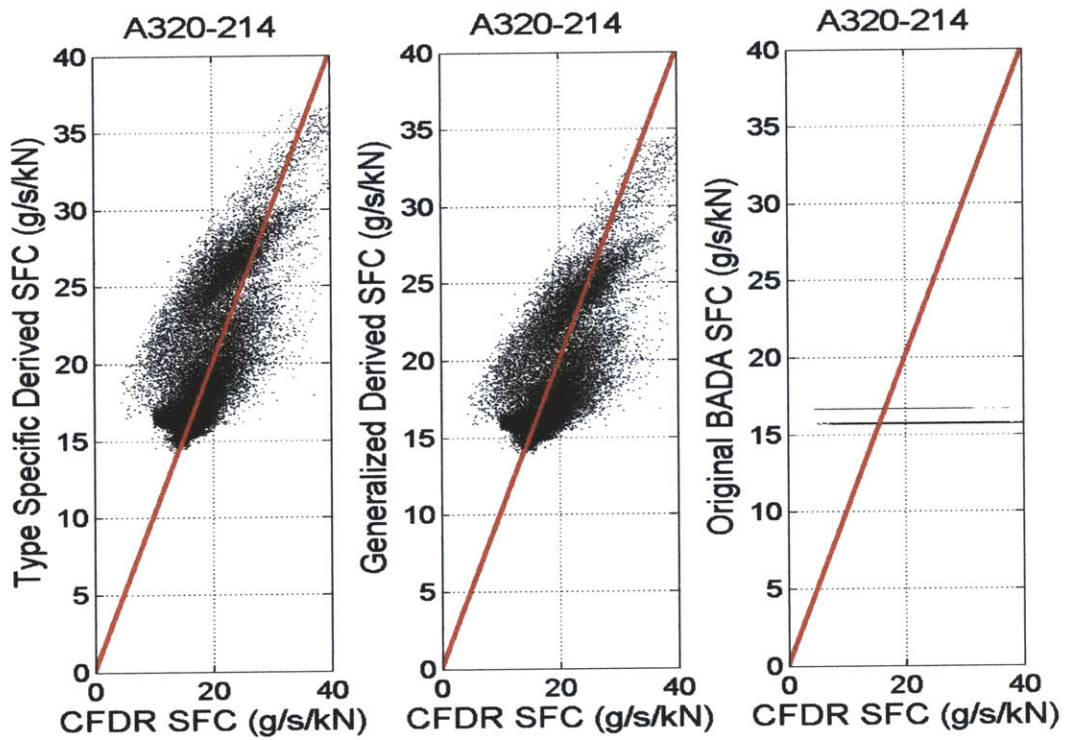


Figure 2.12 – Comparisons of Corrected and Original BADA SFC to CFDR Data (A320-214)

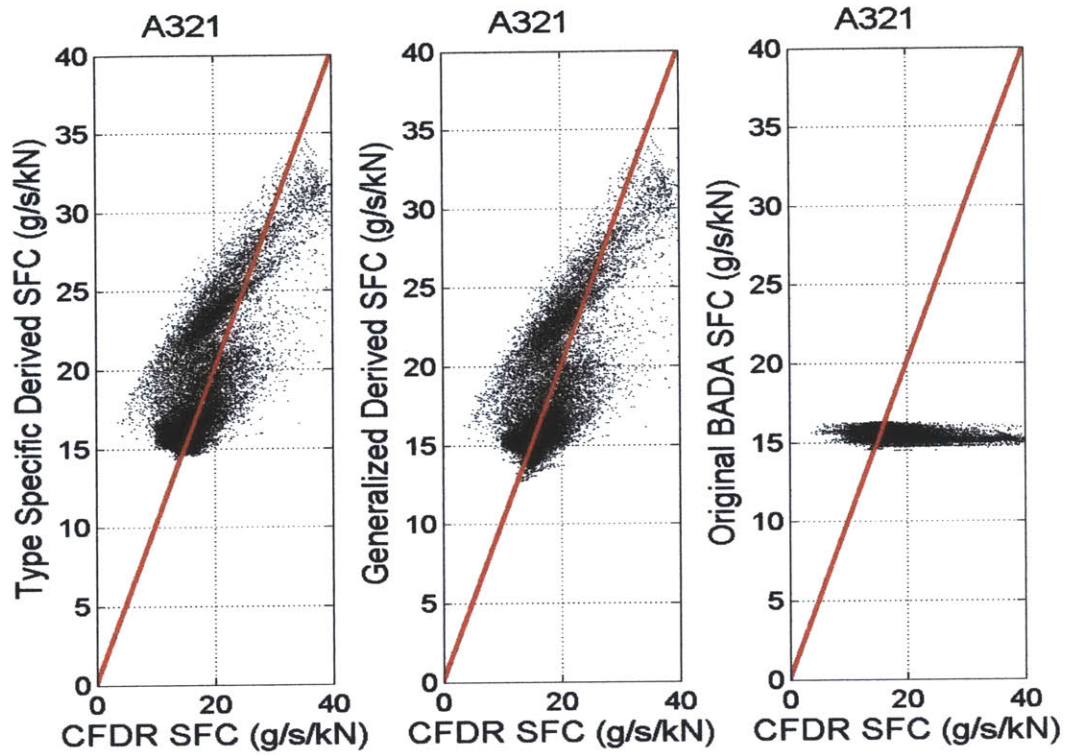


Figure 2.13 – Comparisons of Corrected and Original BADA SFC to CFDR Data (A321)

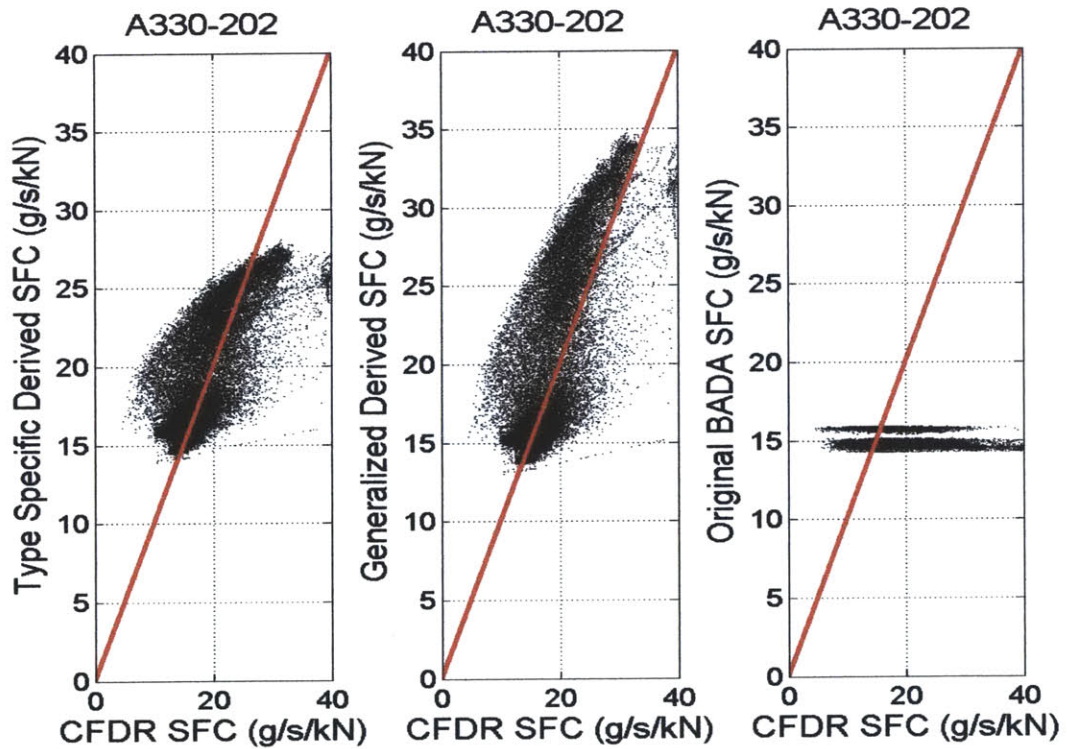


Figure 2.14 – Comparisons of Corrected and Original BADA SFC to CFDR Data (A330-202)

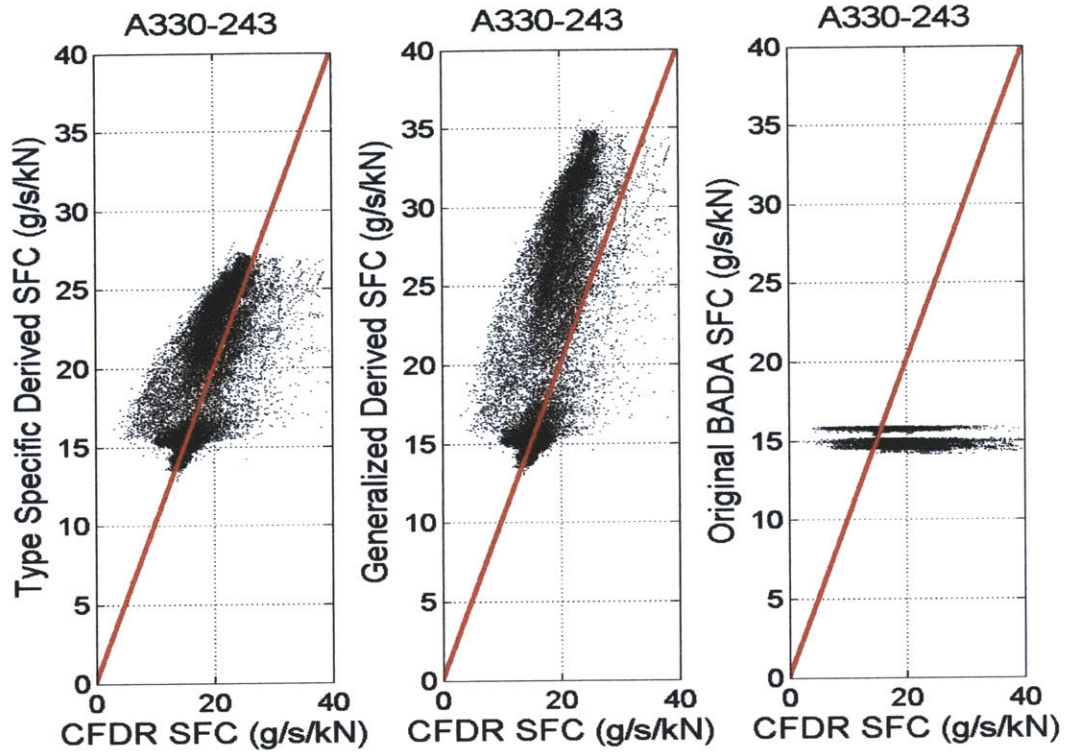


Figure 2.15 – Comparisons of Corrected and Original BADA SFC to CFDR Data (A330-243)

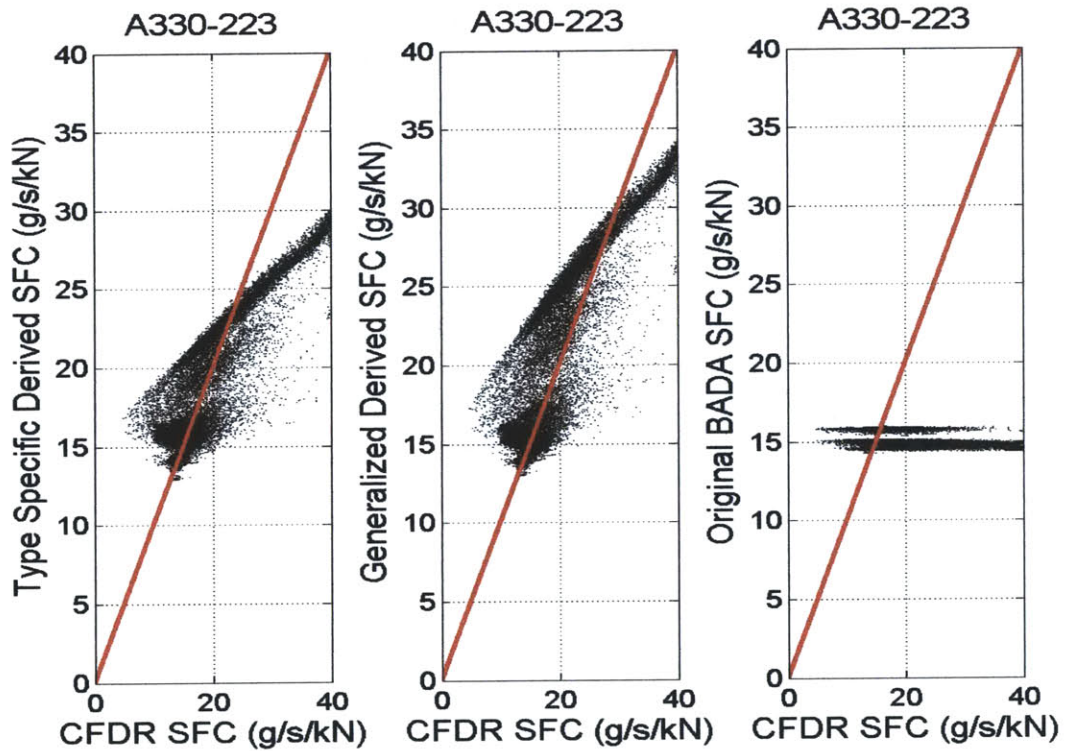


Figure 2.16 – Comparisons of Corrected and Original BADA SFC to CFDR Data (A330-223)

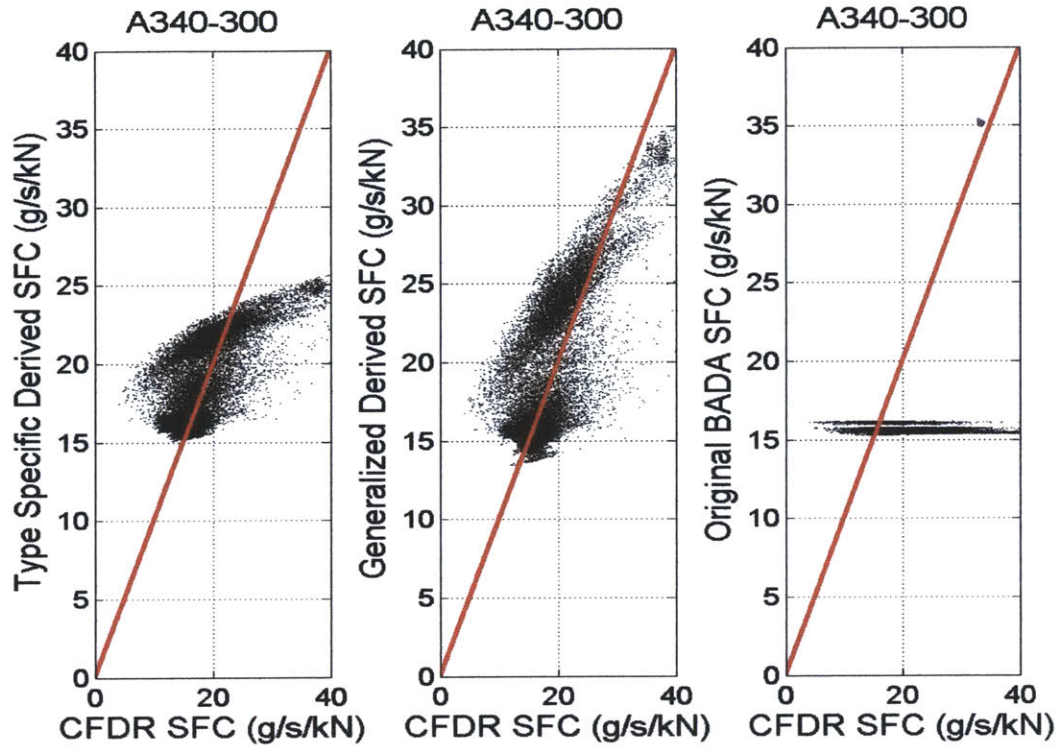


Figure 2.17 – Comparisons of Corrected and Original BADA SFC to CFDR Data (A340-300)

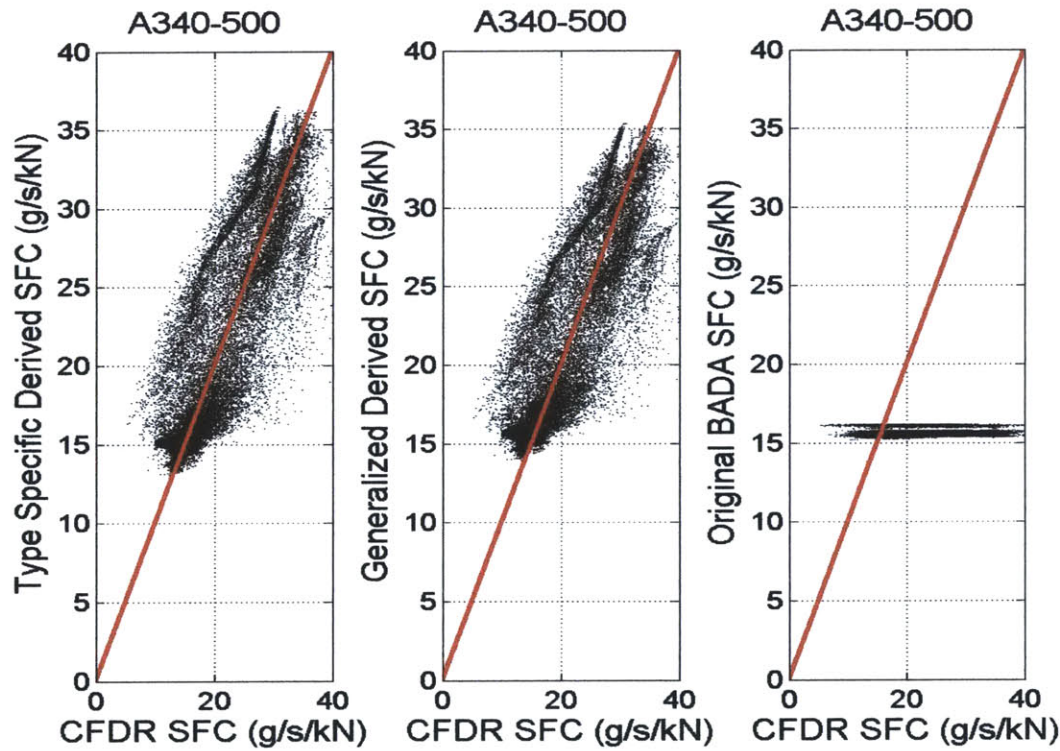


Figure 2.18 – Comparisons of Corrected and Original BADA SFC to CFDR Data (A340-500)

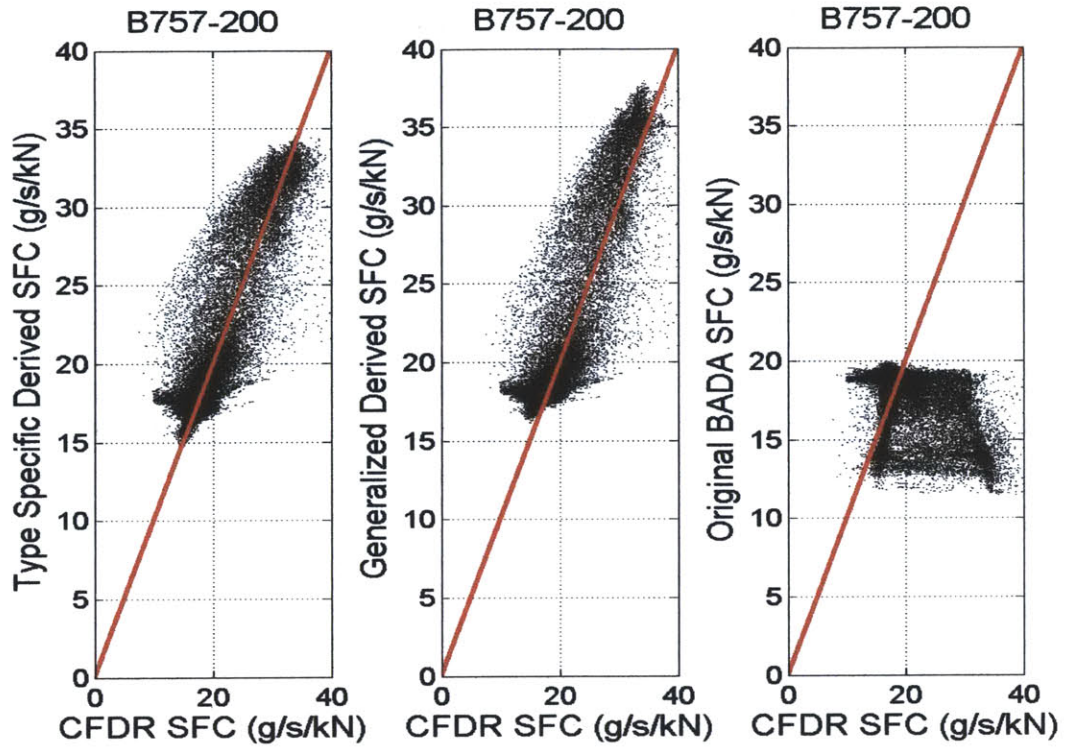


Figure 2.19 – Comparisons of Corrected and Original BADA SFC to CFDR Data (B757-200)

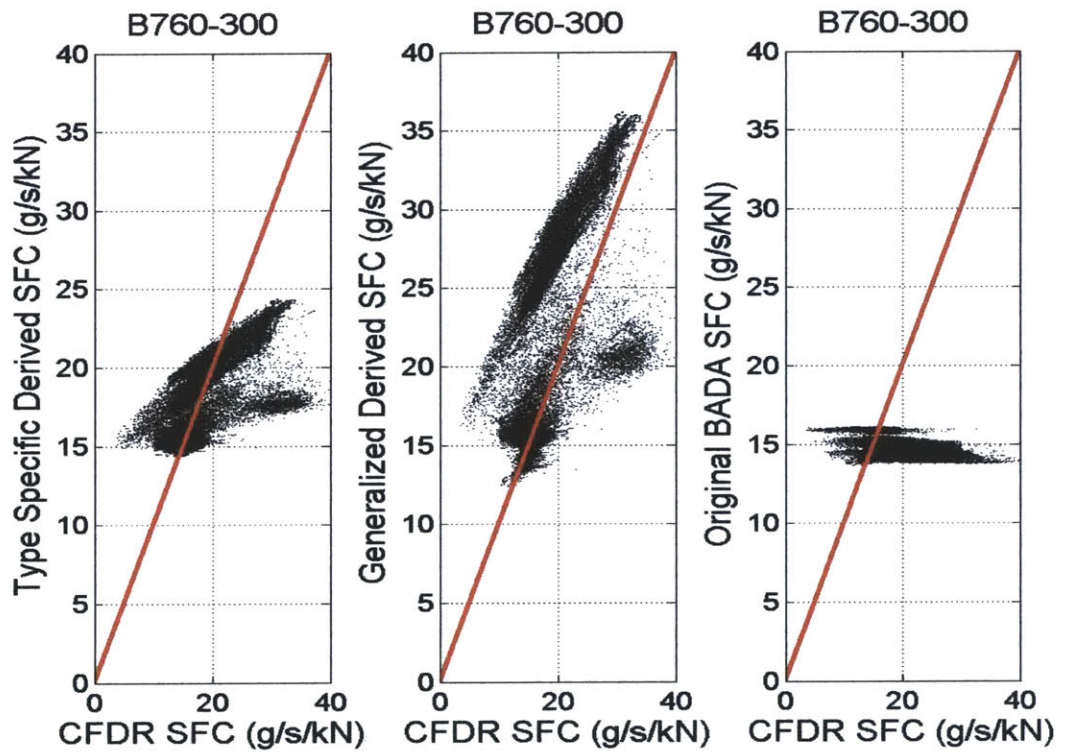


Figure 2.20 – Comparisons of Corrected and Original BADA SFC to CFDR Data (B767-300)

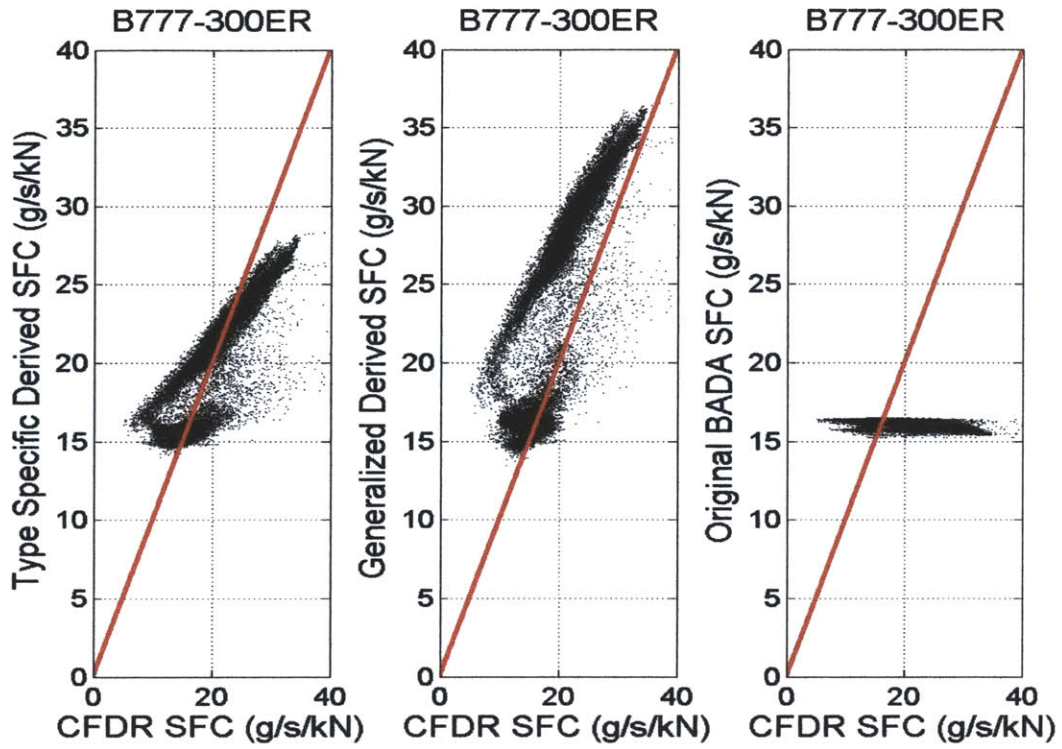


Figure 2.21 – Comparisons of Corrected and Original BADA SFC to CFDR Data (B777-300ER)

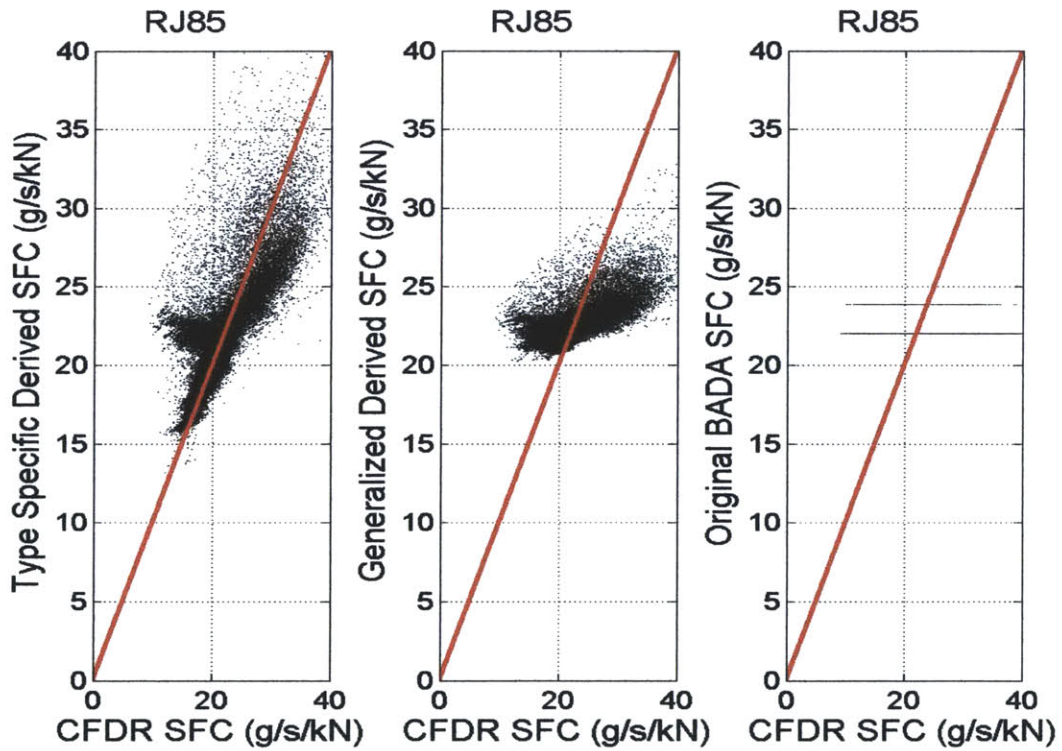


Figure 2.22 – Comparisons of Corrected and Original BADA SFC to CFDR Data (RJ85)

2.3. Inclusion of Meteorological Information

2.3.1. Purpose

The ETMS radar-based trajectories used in SAGE are the result of aircraft flying through the weather that was estimated to exist at that point in space and time. To then model these flights assuming a standard atmosphere and no winds, as was the previous practice in SAGE, introduces error into the performance calculations. In an effort to ameliorate this error, an algorithm was developed to introduce the relevant meteorological information into the calculations.

2.3.2. Approach

The approach taken was to obtain assimilated weather data and then introduce these data into the trajectory and fuel burn calculations. The source of weather data chosen for this purpose was the Goddard Earth Observing System (GEOS)¹⁰ data set available through NASA Goddard Earth Sciences Data and Information Services Center¹¹. This data set is global in coverage and is available from 2000 to present. The spatial resolution of these data is 1° in latitude by 1.25° in longitude and is available at a temporal resolution of 6 hours. The data set, as it was received from NASA, was demarcated at 26 constant pressure levels of 0.01, 0.2, 0.4, 0.5, 0.7, 1, 2, 3, 5, 7, 10, 20, 30, 50, 70, 100, 150, 200, 250, 300, 400, 500, 700, 850, 925, and 1000 hPa, and contained the following variables.

- 1) Ambient Temperature
- 2) U(East) Wind Velocity Component
- 3) V(North) Wind Velocity Component
- 4) Geometric Height (Based on mean sea level datum)

The ETMS trajectories are based upon geometric altitude and it was therefore necessary to preprocess this data set to convert the grid points from constant pressure levels to constant geometric altitude levels. This was a relatively straightforward interpolation process owing to the fact that both the pressure and geometric height were known at each point. The result was a data set with an altitude resolution of 500 m with the additional variable of ambient pressure now given at each altitude. An additional conversion of the U and V wind components into the

wind magnitude and direction was performed to allow for easier assimilation into SAGE. The processed data set then contained the following variables represented at unchanged geographic and temporal resolution and at 500 m demarcations up to an altitude of 20,000 m.

- 1) Ambient Temperature
- 2) Ambient pressure
- 3) Wind Magnitude
- 4) Wind Direction

2.3.3. Implementation

Once the weather data were processed they were stored in a database for use within the trajectory calculations in SAGE. This process is relatively straightforward. At each point along the ETMS trajectories the weather database is interpolated both in space and time. First two sets of three dimensional linear interpolations are carried out in the spatial domain to determine the values of the variables at the two nearest time demarcations available in the database. These values are then interpolated linearly in time to determine the values at the time of the ETMS radar return.

The values of temperature and pressure attained in this manner simply replace the standard atmosphere values that were previously used in SAGE. The incorporation of wind information, however, required the introduction of an additional algorithm. The ETMS data contain groundspeed and heading at each point along the trajectory allowing for the calculation of the true airspeed through an application of the law of cosines as defined below.

$$V_{Airspeed} = \sqrt{(V_{Groundspeed})^2 + (V_{Wind})^2 - 2(V_{Groundspeed})(V_{Wind})\cos(\phi_{Heading} - \phi_{Wind})}$$

The true airspeed was then used in place of groundspeed for all the subsequent performance calculations in SAGE. These include the calculation of drag, thrust, and fuel burn as described in the section 2.1.3.

2.3.4. Results

In an effort to assess the accuracy of the GEOS data set, a comparison was conducted between the values contained in this set and those contained in the CFDR data. The values contained in the CFDR data are in situ measurements as recorded by the aircraft instrumentation and are therefore considered to be a more accurate reflection of reality.

The comparison was accomplished through the same interpolation algorithm utilized in the incorporation of the weather data into SAGE so as to provide an accurate assessment of the fidelity of these data at their end usage. As can be seen in Figures 2.23 through 2.26 the results do indicate a high degree of accuracy in the GEOS data set. These results also provide a validation of the preprocessing and implementation methods as the comparisons were essentially a simulation of these processes.

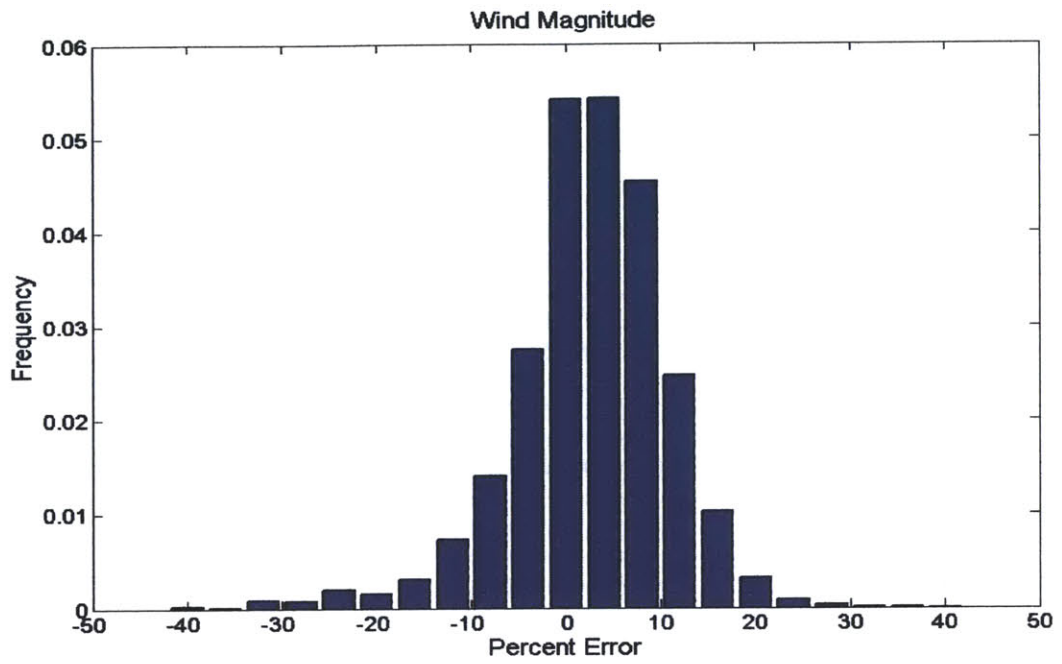


Figure 2.23 – Comparison of GEOS Wind Magnitude to CFDR Data

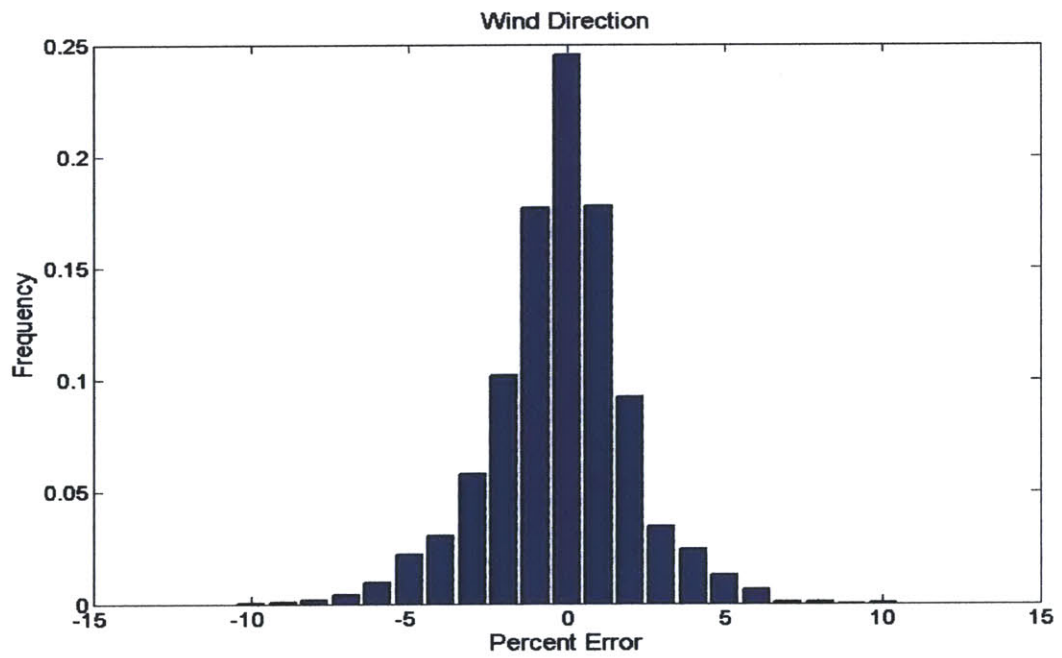


Figure 2.24 – Comparison of GEOS Wind Direction to CFDR Data

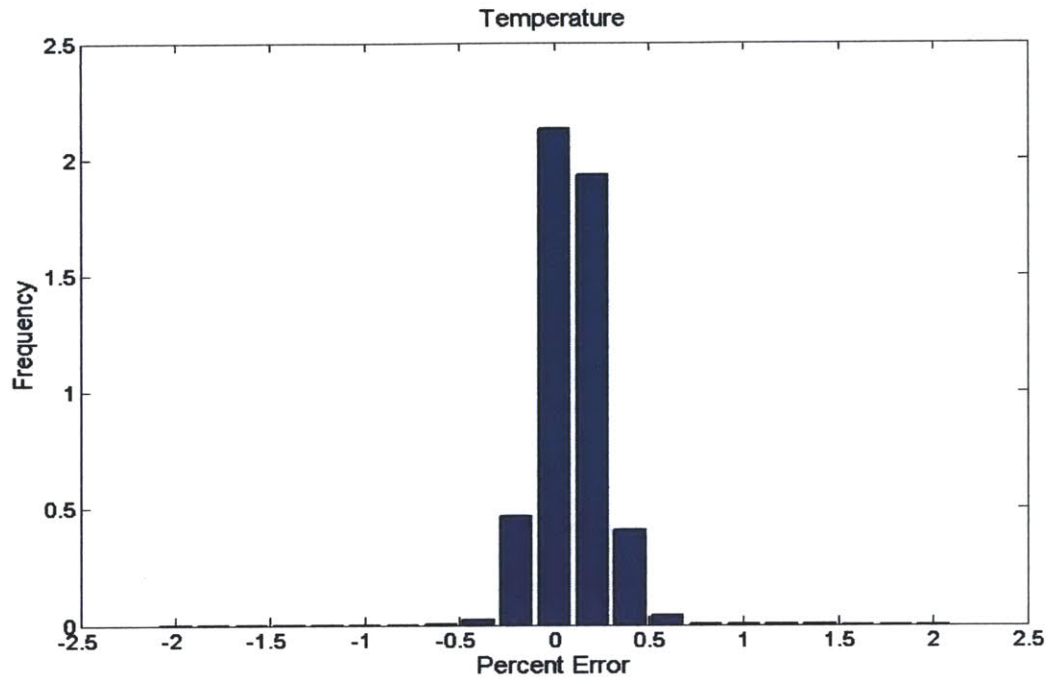


Figure 2.25 – Comparison of GEOS Temperature to CFDR Data

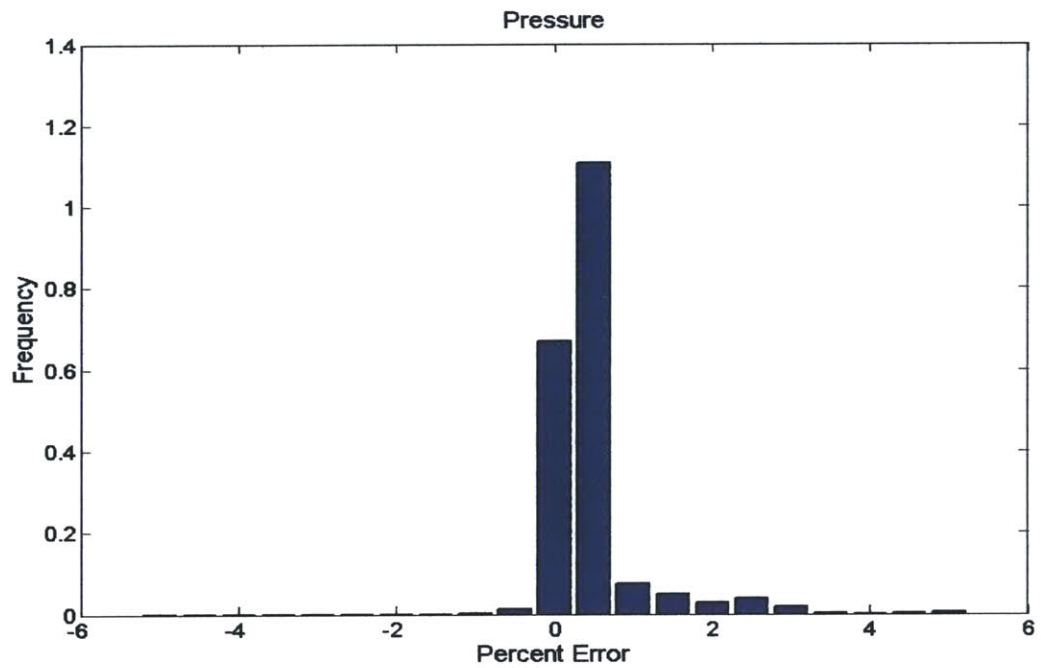


Figure 2.26 – Comparison of GEOS Pressure to CFDR Data

CHAPTER 3: Model Application

3.1. RVSM Benefit Assessment

3.1.1. Purpose

On January 20, 2005 Reduced Vertical Separation Minimums¹² (RVSM) were introduced in airspace over the continental US and southern Canada. Prior to this aircraft operating at altitudes above 29,000 ft were required to maintain a vertical separation of 2000 ft. Following implementation of RVSM this minimum was reduced to 1000 ft which should allow more aircraft to operate closer to optimal cruise altitude as well as decrease the time spent awaiting clearance to cruise altitude. The anticipated results are an increase in capacity as well as an increase in system wide fuel efficiency owing to the increased availability of more optimal cruise altitudes.

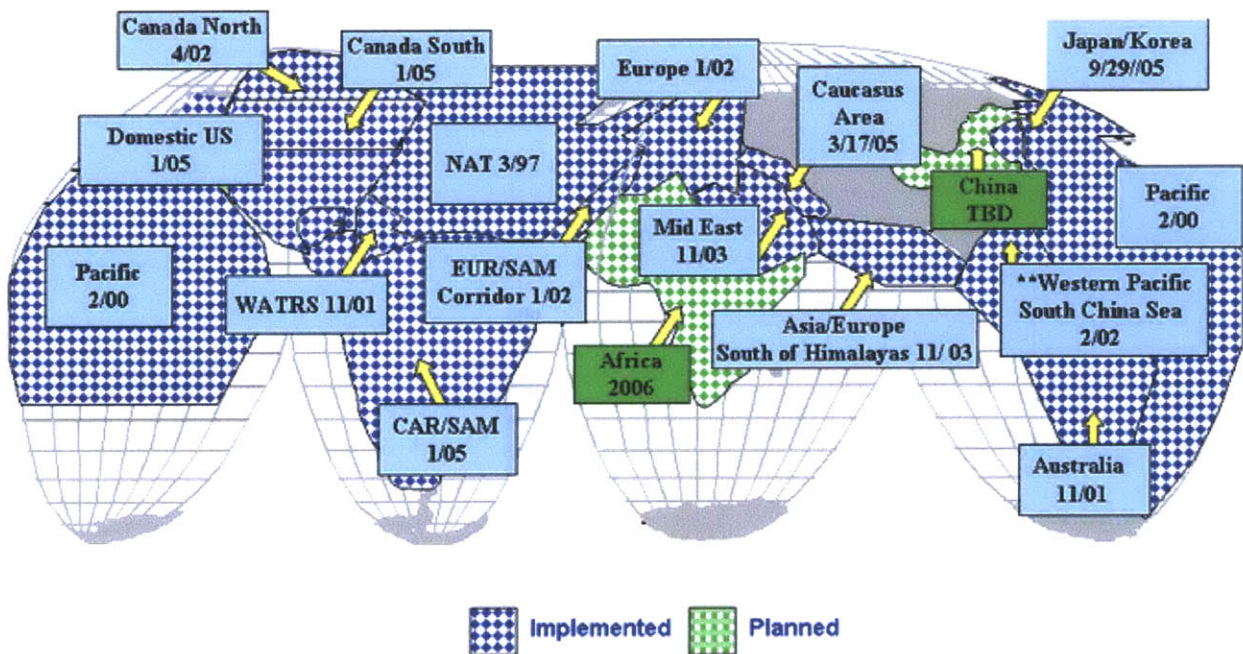


Figure 3.1 – RVSM Implementation Schedule¹⁷

This study is an attempt to quantify the increase in fuel efficiency and the consequent reduction in emissions resulting from the introduction of RVSM in US airspace.

3.1.2. Previous Studies of RVSM

There have been two previous studies investigating the benefits of RVSM.

The first was conducted by EUROCONTROL¹³ and analyzed the impact of RVSM implementation in European airspace which took place on January 24, 2002. This study found a reduction in fuel burn of 1.6% to 2.3% and a reduction in NOx of 0.7% to 1.0% six months after RVSM was implemented. This study made use of radar-based trajectories from 3 days prior to, and 6 days following RVSM. These radar trajectories were analyzed using the Advanced Emission Model¹⁴ (AEM3) developed by EUROCONTROL, a modeling methodology similar to that employed in SAGE. This analysis was conducted under the assumption of standard atmospheric conditions and no winds.

The second was published by the FAA¹⁵ in September 2005 and analyzed the impact of RVSM implementation in the US. This study was constrained to the traffic between the following twelve city pairs.

LAX-JFK	ATL-DEN	ORD-MIA	IAH-EWR	DTW-DFW	MIA-EWR
MSP-DTW	ORD-LGA	IAD-MCO	PHX-IAH	DFW-IAD	DFW-LGA

The dates covered by this study are given in Table 3.1 on the following page. These dates and city pairs were cited as being representative of the normal traffic load and geographic distribution of flights within the National Airspace System (NAS) and the data used in the comparison were obtained from the Performance Data Analysis and Reporting System (PDARS)¹⁶. This report concluded that, based upon BADA tables, the fleet averaged fuel burn was reduced by approximately 3 lbs per minute while en-route at the more optimal cruise altitudes available under RSVM. The average increase in cruise altitude was found to be 380 ft. Additionally, the added routing flexibility under RSVM allowed aircraft to remain at cruise altitude an average of 2.5 minutes longer, resulting in an average fuel savings of 20-25 lbs per flight.

3.1.3. Approach

The general approach taken was to make use of SAGE processed ETMS trajectories from representative periods prior to and following the implementation of RVSM to assess the system wide change in efficiency. The same representative periods used in the previous FAA study were used in this analysis given that they are considered to be periods of normal traffic load in the NAS. These dates are given in Table 3.1, below.

Table 3.1– Dates Examined in RVSM Study¹⁵

	Dates	Days
Pre-DRVSM	11/14/2004 - 11/20/2004	7
	12/05/2004 - 12/18-2004	14
	1/9/2005 - 1/15/2005	7
	Pre-DRVSM Total	28
Post-DRVSM	2/13/2005 - 3/12/2005	28
	Post-DRVSM Total	28
	Grand Total	56

In order to ensure comparability between the pre- and post-RVSM results, the ETMS flights were filtered by flight ID, origin-destination pair, and aircraft type. All flights during one period which could not be matched according to these criteria to an analogous flight in the other period were dropped from the study. Additionally, the remaining flights were separated into two subsets, namely, those originating or terminating internationally and those which were entirely US domestic flights.

These filtered flights were then modeled in SAGE and the fuel burn and emissions results were analyzed to determine any changes in efficiency. This analysis was conducted under four combinations of modeling assumptions and efficiency metrics.

- 1) Original BADA fuel burn model. Standard Atmosphere. Ground distance efficiency.
- 2) Original BADA fuel burn model. GEOS weather data. Ground distance efficiency.
- 3) CFDR derived fuel burn model. GEOS weather data. Ground distance efficiency.
- 4) CFDR derived fuel burn model. GEOS weather data. Air distance efficiency.

Methods one, two, and three make use of a ground distance efficiency metric which is indicative of the fuel burn and emissions per ground distance traveled. Analysis under this metric was relatively straightforward as SAGE outputs include fuel burn, emissions, and ground distance for each flight segment that is modeled. These quantities were summed over all the chords modeled for the period in question and divided to arrive at the global efficiency for that period. The definition of ground distance efficiency for a given study period was defined as the sum of the ground distances over the sum of the fuel burn.

$$\eta = \frac{\sum \Delta X_{Ground}}{\sum m_f}$$

Method four makes use of an air distance efficiency metric. Since the variation in wind patterns between the pre and post RVSM study periods is significant, it was determined that a more accurate indication of efficiency would be provided by this metric. (Figures 3.2 and 3.3 depict the substantial shift in location and intensity of cruise altitude winds between the two study periods as indicated by the GEOS data set.) The idea here was to use the air distance, or the distance the aircraft actually traveled through the air, instead of the ground distance in order to normalize out the effects of wind variations. Analysis under this metric required post processing of the segment level outputs to convert the ground distances to air distances through the following relation,

$$\Delta X_{Air} = \Delta X_{Ground} \frac{V_{Airspeed}}{V_{Groundspeed}}$$

Under the air distance efficiency metric the efficiency for a given period is defined as,

$$\eta = \frac{\sum \Delta X_{Air}}{\sum m_f}$$

The change in efficiency, $\Delta\eta$, resulting from the implementation of RVSM was calculated as a fractional change for each of the study methods according to the relation,

$$\Delta\eta = \frac{\eta_{post} - \eta_{pre}}{\eta_{pre}}$$

Thus a positive $\Delta\eta$ is indicative of an increase in efficiency.

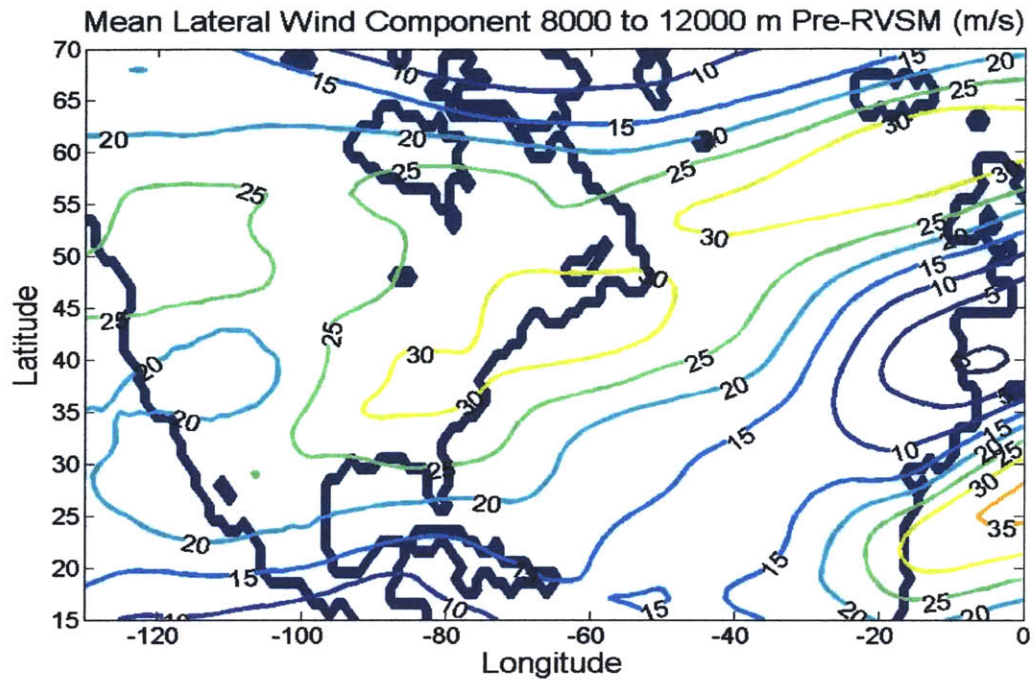


Figure 3.2 – Cruise Altitude Winds during Pre-RVSM Study Period

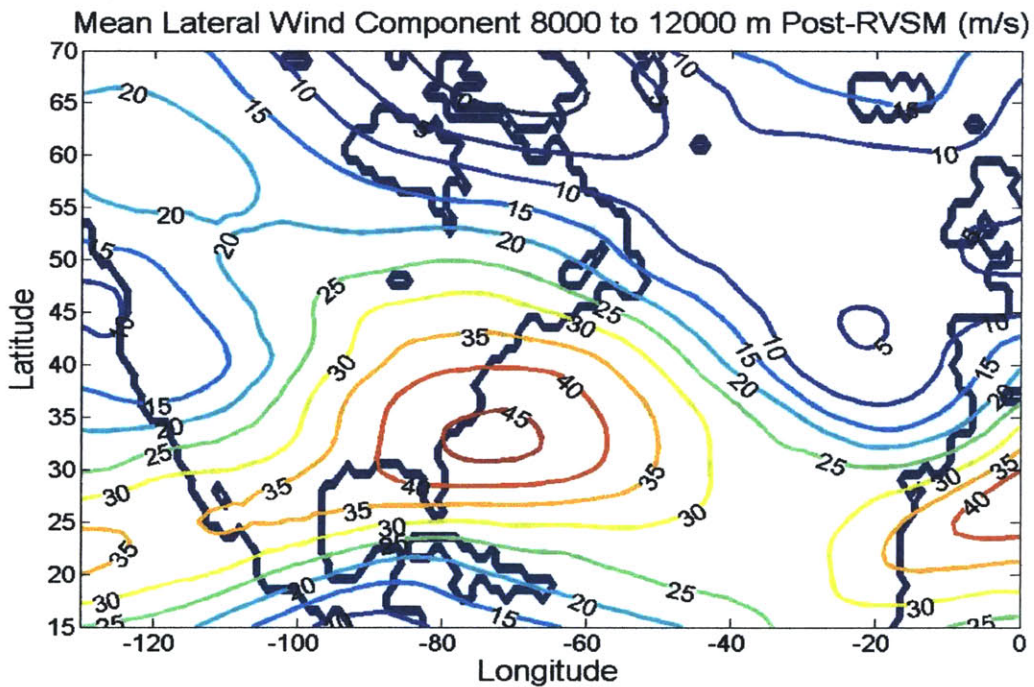


Figure 3.3 – Cruise Altitude Winds during Post-RVSM Study Period

In an effort to substantiate the accuracy of the US domestic comparison, an additional comparison was conducted using ETMS data from the international subset within North Atlantic and E.U. airspace. This comparison was limited to fuel burn and was conducted under analysis methods 3 and 4. In theory this control comparison should not indicate any change in efficiency between the study periods as RVSM was implemented over the North Atlantic in March 1997 and over Europe in January 2002¹⁷. Figures 3.4 and 3.5 depict the ETMS data points used in the US domestic analysis and Figures 3.6 and 3.7 depict the ETMS data points used in the control analysis.

There was also a desire to estimate the variability of the results associated with the choice of time periods under study. To this end, both of the original 28 day study periods were divided into two 14 day periods. The first two week period of the Pre-RVSM scenario (11/14/2004-11/20/2004 and 12/05/2004-12/11/2004) was compared against the first two week period of the Post-RVSM scenario (12/13/2005-2/26/2005); and the second two week period of the Pre-RVSM scenario (12/12/2004-12/18/2004 and 1/9/2005-1/15/2005) was compared against the second two week period of the Post-RVSM scenario (2/27/2005-3/12/2005). The results of these two sub-analysis differed somewhat from the aggregate results and were taken as an estimate of the potential variability and are included as error bars on the aggregate results in the following section.

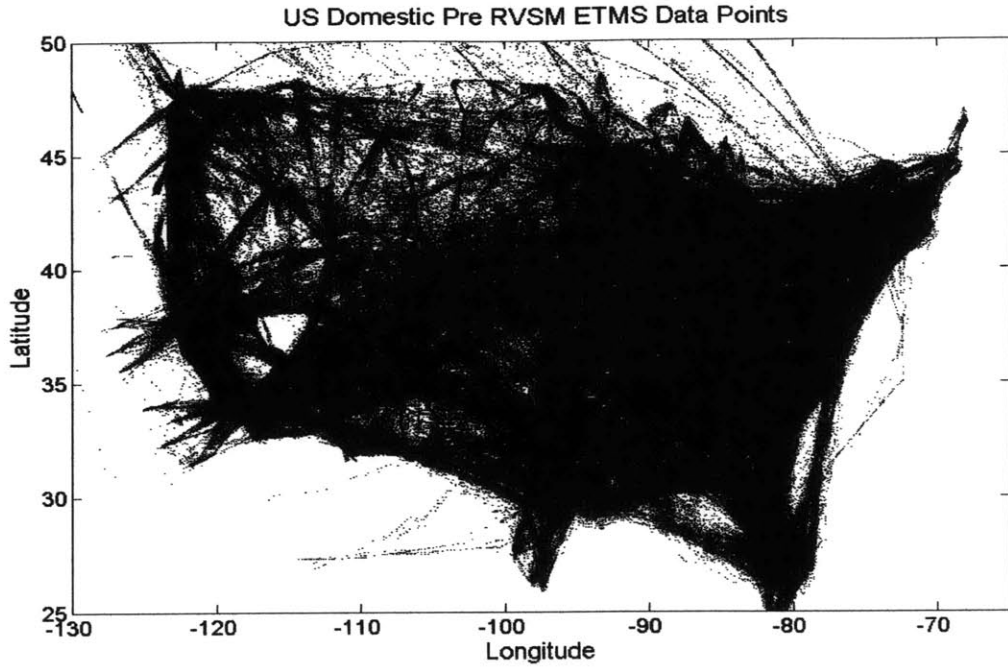


Figure 3.4 – US Domestic Pre RVSM ETMS Data Points

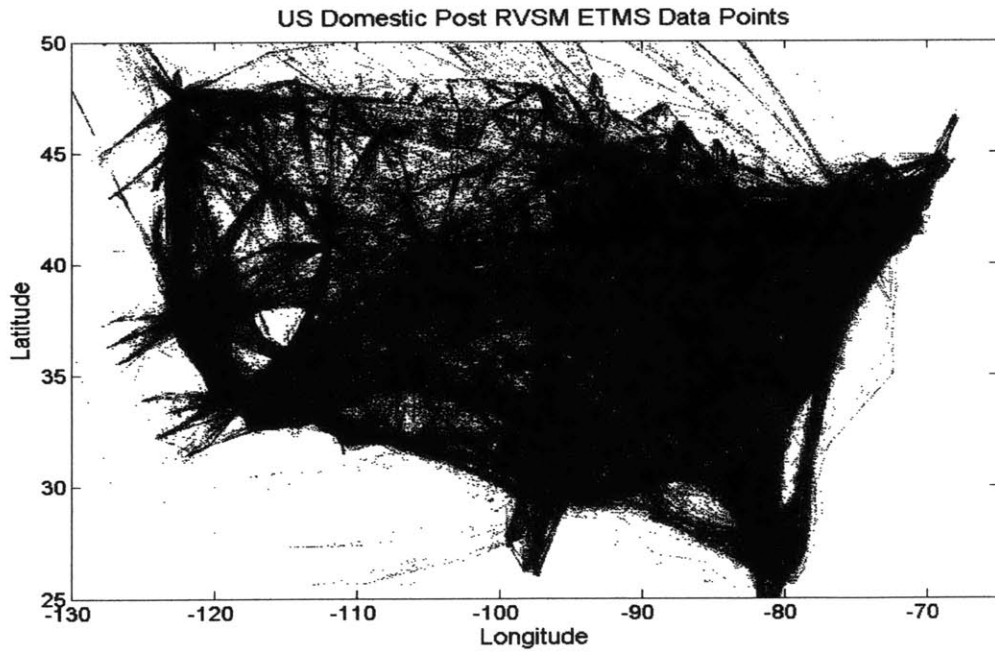


Figure 3.5 – US Domestic Post RVSM ETMS Data Points

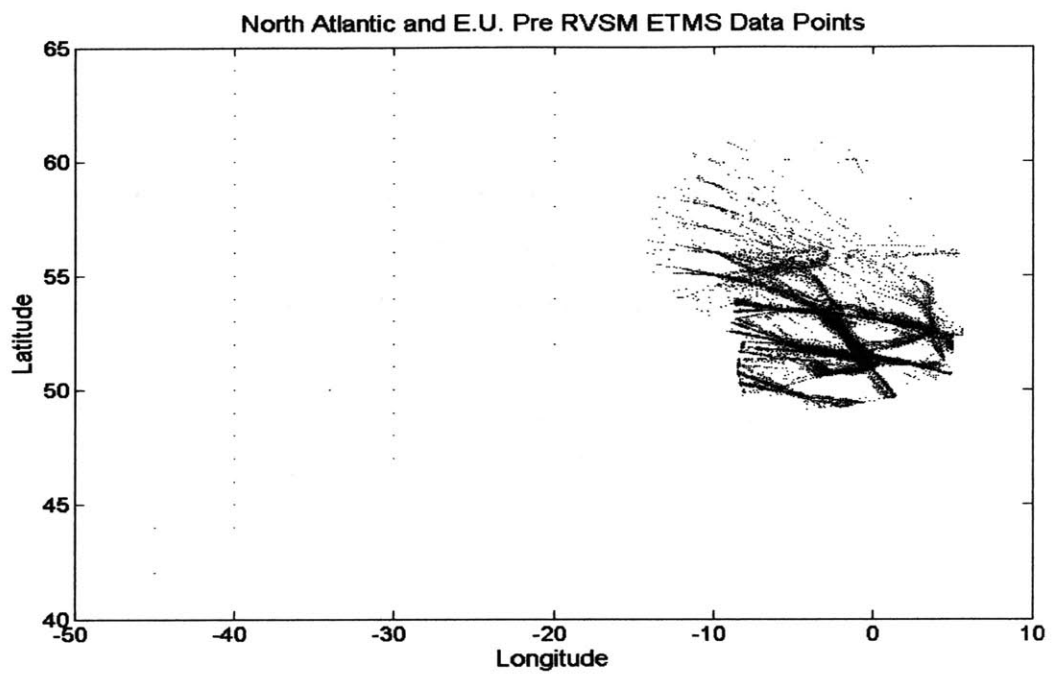


Figure 3.6 – North Atlantic and E.U. Pre RVSM ETMS Data Points

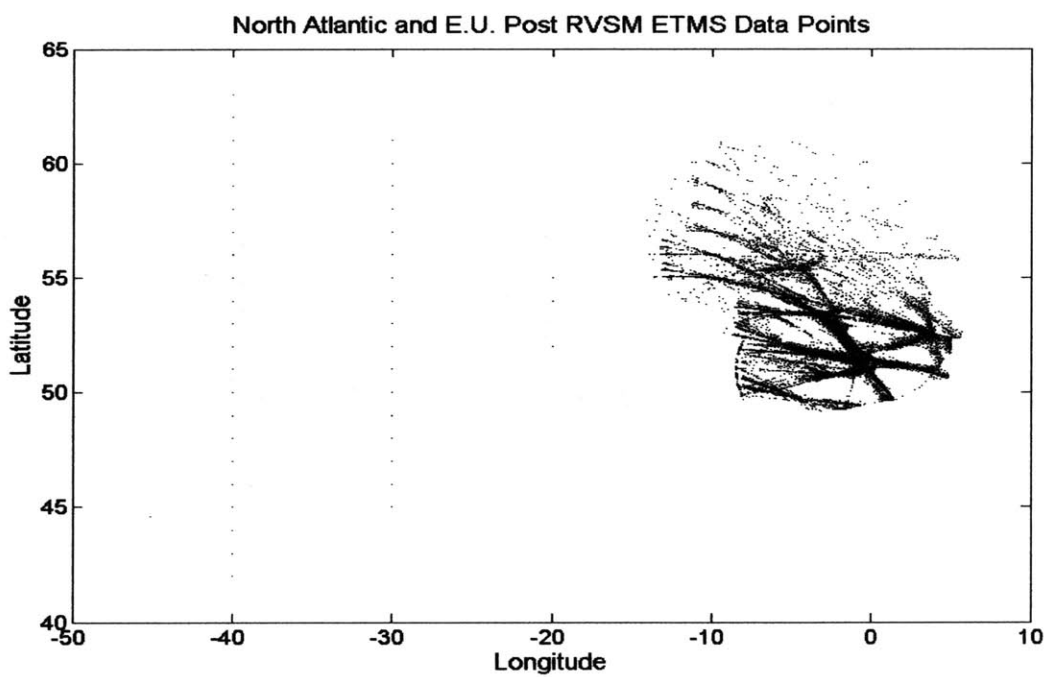


Figure 3.7 – North Atlantic and E.U. Post RVSM ETMS Data Points

3.1.4. Results

The results of the US domestic analysis are presented numerically in Table 3.2 and graphically in Figure 3.8 for each of the four previously mentioned analysis methods.

- 1) Original BADA fuel burn model. Standard Atmosphere. Ground distance efficiency.
- 2) Original BADA fuel burn model. GEOS weather data. Ground distance efficiency.
- 3) CFDR derived fuel burn model. GEOS weather data. Ground distance efficiency.
- 4) CFDR derived fuel burn model. GEOS weather data. Air distance efficiency.

Table 3.2– US Domestic RVSM Analysis Results

Analysis Method	1		2		3		4	
	Pre	Post	Pre	Post	Pre	Post	Pre	Post
Number of Flights	218335	218335	218335	218335	218335	218335	218335	218335
Total Distance (nm)	1.237E+08	1.238E+08	1.235E+08	1.236E+08	1.235E+08	1.236E+08	1.240E+08	1.243E+08
Total Fuel Burn (kg)	8.737E+08	8.733E+08	8.785E+08	8.672E+08	8.430E+08	8.298E+08	8.430E+08	8.298E+08
Total NOx (kg)	1.143E+07	1.137E+07	1.161E+07	1.134E+07	1.082E+07	1.051E+07	1.082E+07	1.051E+07
$\Delta\eta$ Fuel Burn (%)	0.14		1.31		1.61		1.81	
$\Delta\eta$ NOx (%)	0.59		2.35		2.94		3.14	

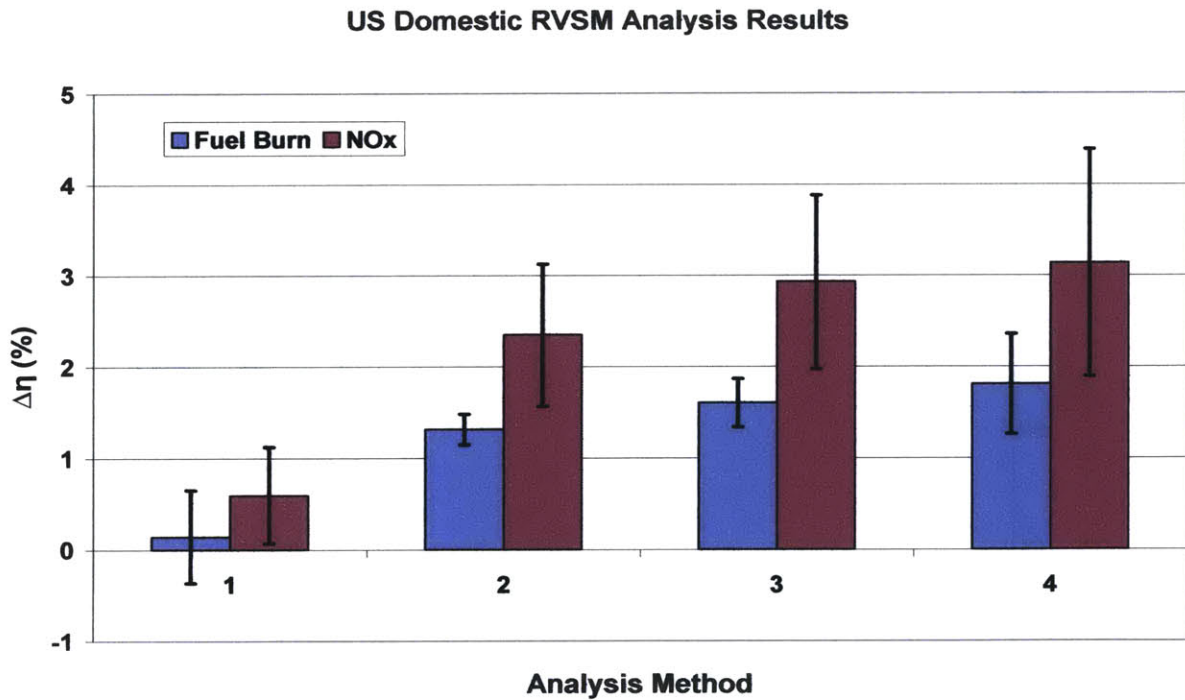


Figure 3.8 – US Domestic RVSM Analysis Results

As can be seen in the large difference between methods one and two, the introduction of weather data had the greatest impact on the results. The introduction of weather into the analysis accounted for 65% of the reported RVSM fuel burn benefit. The inclusion of the additional functionality derived from the CFDR data in the SFC model also had a significant impact as evidenced by the difference between methods two and three. This use of the generalized derived SFC model accounted for 17% of the reported benefit in fuel burn. The use of the air distance efficiency metric in method four also had some impact on the results, accounting for 11% of the reported fuel burn benefit. The fact that the use of the air distance efficiency metric did not have a larger impact is likely attributable to the fact that the flights in the US domestic comparison vary widely in heading. Thus, in aggregate the effects of wind are largely negated.

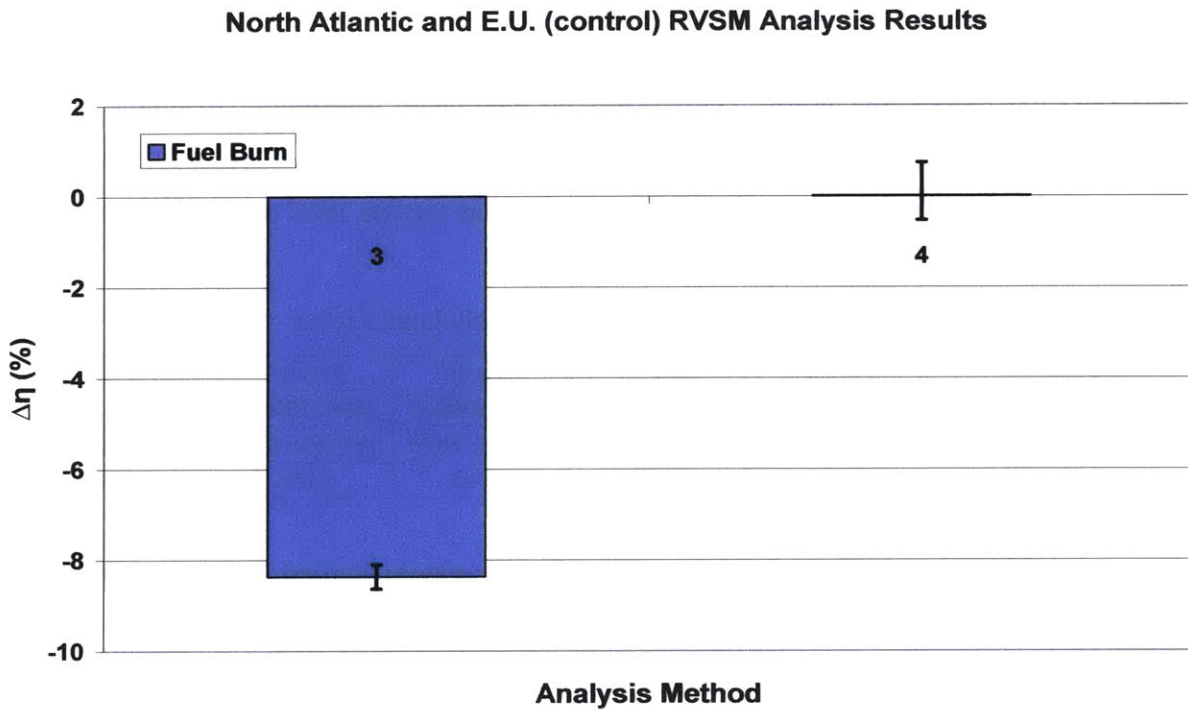


Figure 3.9 – North Atlantic and E.U. (control) RVSM Analysis Results

The control comparison of the North Atlantic and E.U. region resulted in a nearly zero efficiency change under method four as indicated in Figure 3.9. In this case, the large difference in the results of methods three and four is due to the fact that the flights examined

are nearly all heading East (inbound to the E.U.). Thus the difference in wind velocity between the two study periods appears as a substantial loss of efficiency under method three which is based on the ground distance efficiency metric. Using the air distance efficiency metric of method four resulted in a $\Delta\eta$ of only .012%, lending credence to this metric being the more appropriate of the two and providing support for the results of the US domestic analysis under method four .

An additional factor to consider regarding this analysis is the possible effect of aircraft load factor. A rational metric to use in evaluating efficiency is the fuel required to transport a given mass over a given distance. In the context of this study, such an efficiency metric would be defined,

$$\eta = \frac{\sum (m_p \Delta X)}{\sum m_f}$$

Unfortunately, system wide information on payload is not available at the level of resolution necessary to evaluate this metric. There is aircraft load factor information available in monthly aggregate as reported by air carriers to the FAA through Form 41¹⁸ reporting requirements. The Form 41 reported load factors, which are defined as ton-km used per ton-km available, are presented in table 3.3.

Table 3.3– US Domestic Monthly Load Factors

	Nov-04	Dec-04	Jan-05	Feb-05	Mar-05
ton-km avail	30818932929	32881939723	30639840565	28993559607	33189372214
ton-km Used	16578983854	18475980217	16639218070	16126964011	20068370309
load factor	0.538	0.562	0.543	0.556	0.605

These monthly aggregate load factors could not be accurately applied in this analysis since the periods being considered are only portions of each month and purposefully exclude periods of increased holiday travel. It does appear that the average load factor during post-RVSM months is slightly greater than those during pre-RVSM months, and thus, if this efficiency metric were used to evaluate RVSM an increase in the benefit would likely be realized.

3.1.5. Conclusions

The results of this study indicate that the implementation of RVSM in US Domestic airspace did result in a quantifiable increase in system wide efficiency. The reported value of this increase varied amongst the four different analysis methods, though all methods indicate a positive shift in efficiency.

The inclusion of weather information had a significant impact on the results. It was found that neglecting winds leads to an average absolute error in true airspeed of around 10%, and thus inclusion of this information provides a more accurate assessment.

The inclusion of a SFC model which contains the relevant functional dependence on ambient and operational variables was also found to contribute positively to the results of this study. The results presented in section 2.1 indicate that there is a significant improvement in model fidelity obtained through the use of this model.

The results of the control comparison indicate that the air distance metric is an adequate means of accounting for variations in prevailing winds, and thus method four, an air distance metric using meteorological information and the revised SFC model, is believed to provide the highest degree of accuracy in assessing RVSM benefits.

Therefore, the conclusion of this study is that the implementation of RVSM in US Domestic airspace resulted in an increase in fuel efficiency of 1.81% ($\pm 0.55\%$) and an increase in NOx efficiency of 3.14% ($\pm 1.25\%$).

APPENDIX A: Example

A.1. Transonic Drag Correction

The algorithm used to determine the transonic drag rise is based upon the method developed by Ilan Kroo (Stanford) and adapted for use in AEDT/SAGE by Kelly Klima. A more in depth description of the adaptation process can be found in Kelly's thesis¹⁹. A description of the final algorithm is given here.

$$X = \frac{M}{M_{BC}}$$

$$Y = X - 1$$

if $X \geq 1$

$$\Delta C_d = .001 + .02727Y - .1952Y^2 + 19.09Y^3$$

if $1 > X \geq .95$

$$\Delta C_d = .001 + .02727Y + .4920Y^2 + 3.573Y^3$$

if $.95 > X \geq .8$

$$\Delta C_d = .0007093 + .006733Y + .01956Y^2 + .01185Y^3$$

if $.8 > X \geq .5$

$$\Delta C_d = .00013889 + .00055556Y + .00055556Y^2$$

if $.5 > X$

$$\Delta C_d = 0$$

REFERENCES

- ¹ Penner, J., et al., “*Aviation and the Global Atmosphere*”, Summary for Policy Makers, Intergovernmental Panel on Climate Change, 1999. [http://www.ipcc.ch/pub/av\(E\).pdf](http://www.ipcc.ch/pub/av(E).pdf)
- ² FAA, “*SAGE Technical Manual*”, Office of Environment and Energy, Version 1.5, 2005
http://www.faa.gov/about/office_org/headquarters_offices/aep/models/sage/media/FAA-EE-2005-01_SAGE-Technical-Manual.pdf
- ³ FAA, <http://hf.tc.faa.gov/projects/etms.htm>
- ⁴ Nuic, A. “*User Manual for Base of Aircraft Data (BADA)*”, Eurocontrol Experimental Centre, Cedex, France, revision 3.6 edition, July 2004.
http://www.eurocontrol.int/eec/gallery/content/public/documents/EEC_notes/2004/EEC_note_2004_10.pdf
- ⁵ Baughcum, S. L., et al. “*Scheduled Civil Aircraft Emissions Inventories for 1992: Database Development and Analysis, Appendix D: Boeing Method 2 Fuel Flow Methodology Description.*” Report NASA CR 4700, The Boeing Company, April 1996.
- ⁶ UK CAA, <http://www.caa.co.uk/default.aspx?categoryid=702&pagetype=90>
- ⁷ Polymeris, J., Swiss Flight Data Monitoring, CH-8058 Zurich
- ⁸ Malwitz, A, et all, “*SAGE Version 1.5 Validation Assessment Model Assumptions and Uncertainties*”, Federal Aviation Administration, Office of Environment and Energy,
http://www.faa.gov/about/office_org/headquarters_offices/aep/models/sage/media/FAA-EE-2005-03_SAGE-Validation.pdf
- ⁹ Hill and Peterson, “*Mechanics and Thermodynamics of Propulsion*”, Second Edition, Addison-Wesley, 1992.
- ¹⁰ Suarez, Max, Editor, “*Documentation and Validation of the Goddard Earth Observing System (GEOS) Data Assimilation System*”, Version 4, April 2005,
<http://gmao.gsfc.nasa.gov/pubs/docs/Bloom168.pdf>
- ¹¹ NASA Goddard Space Flight Center “Global Modeling and Assimilation Office,”
<http://gmao.gsfc.nasa.gov/index.php> , 2006.
- ¹² FAA, <http://www.faa.gov/ats/ato/rvsm1.htm>
- ¹³ Jelinek, F., Carlier, S., et. all, “*The EUR RVSM Implementation Project Environmental Benefit Analysis*,” EEC/ENV/2002/008, October 2002.
http://www.eurocontrol.int/eec/gallery/content/public/documents/EEC_SEE_reports/EEC_SEE_2002_008.pdf
- ¹⁴ Carlier, S. “*GAES - Advanced Emissions Model (AEM3) v1.5 - Validation Exercise #4*” ENVISA, 2006
http://www.eurocontrol.int/eec/gallery/content/public/documents/EEC_SEE_reports/EEC_SEE_2006_007.pdf

¹⁵ CDM/ DRVSM Work Group Report, “*Benefit Analysis and Report for Domestic Reduced Vertical Separation Minimum (DRVSM)*,” FAA Air Traffic Organization System Operations Services, September 2005.

http://cdm.fly.faa.gov/Workgroups/DRVSM/2005/DRVSM_BenefitReport_091405.doc

¹⁶ <http://pdars.arc.nasa.gov/>

¹⁷ FAA Air Traffic Organization “RVSM Status Worldwide,”

http://www.faa.gov/ats/ato/status_ww.htm , 2005.

¹⁸ Bureau of Transportation Statistics, U.S. Department of Transportation.

http://www.transtats.bts.gov/databases.asp?Mode_ID=1&Mode_Desc=Aviation&Subject_ID2=0

¹⁹ Klima, K., “*Assessment of Global Contrail Modeling Method and Operational Strategies for Contrail Mitigation*”, Massachusetts Institute of Technology, 2005.